Title page

Title: Sterol-O acyltransferase 1 is inhibited by gga-miR-181a-5p and gga-miR-429-3p through the TGFβ pathway in endodermal epithelial cells of Japanese quail

Short title: microRNAs regulate SOAT1 in EECs

Han-Jen Lin[1¶], Chiao-Wei Lin[2&], Harry J. Mersmann[1&], Shih-Torng Ding[1,2*].

¶ 1st set of equal contributors.

& 2nd set of equal contributors, these authors also contributed equally to this work.

***Corresponding author:** Dr. Shih-Torng Ding (sding@ntu.edu.tw).

[1]Department of Animal Science and Technology, National Taiwan University, Taipei City, Taiwan (R.O.C.).

[2]Institute of Biotechnology, National Taiwan University, Taipei City, Taiwan (R.O.C.).

Mailing address: No.50, Ln. 155, Sec. 3, Keelung Rd. Sec. 3, Taipei City 106, Taiwan (R.O.C.)

Tel number: +886-2-3366-4175

Fax number: +8862-2732-4070

Abstract

Nutrients are utilized and re-constructed by endodermal epithelial cells (EECs) in yolk sac membranes in avian species. Sterol-O acyltransferase 1 (SOAT1) is the key enzyme to convert cholesterol to cholesteryl ester for delivery to growing embryos. During development, absorption of yolk is matched with significant changes of SOAT1 mRNA and enzyme activity. miRNAs regulate angiogenesis and metabolism during mammalian development. However, the involvement of miRNAs in lipid utilization during avian embryogenesis remains ambiguous.

Using a miRNA sequencing technique, we found several candidate miRNAs and confirmed expression patterns with real time PCR. They were selected for as candidates targeting the receptor (TGFβ receptor type 1, TGFBR1) that may regulate SOAT1. Similar to SOAT1 mRNA accumulation, the gga-miR-181a-5p expression was gradually elevated during development, but the concentration of gga-miR-429-3p was in the opposite direction. Transfection with gga-miR-181a-5p or gga-miR-429-3p inhibited TGFBR1 and SOAT1 in EECs. The 3' untranslated region (3'UTR) of TGFBR1 was then confirmed to be one of the targets of gga-miR-181a-5p and gga-miR-429-3p. Taken together, expression of miRNAs during embryonic development regulates SOAT1 expression by inhibiting the 3'UTR of TGFBR1. This is indicative of possible regulation of avian yolk lipid utilization

and modification of hatchability by changing miRNA expressions.

Introduction

SOAT1 (sterol-O acyltransferase 1), also named ACAT1 (acyl-Coenzyme A: cholesterol acyltransferase 1), is the key enzyme to catalyze cholesterol conversion into cholesteryl ester, by adding fatty acyl coenzyme A; thus, a less polar molecule is produced [1]. Yolk sac membrane (YSM), a three-layer extraembryonic tissue, serves crucial roles for avian embryos during the entirety of embryonic development. We demonstrated that SOAT1 activity in endodermal epithelial cells (EECs, the third layer of YSM) was activated by specific nutrients and hormones through the cAMP-dependent PKA signaling pathway, and accumulated more cholesterol ester in EECs [2].

The diversity of bio-functions and involvement of non-coding RNAs has raised considerable issues. Non-coding RNAs include short (microRNAs, miRNAs) and long non-coding (lncRNAs), ribosomal (rRNAs), transfer (tRNAs), small nuclear (snRNAs), small nucleolar (snoRNAs), transfer-messenger (tmRNAs) and telomerase RNAs [3]. The functions and regulations of miRNAs have been examined in mammalian species for decades. Mainly, mature miRNAs are paired to 3' untranslated regions (UTR) or 5'UTR by identifying seed regions of target genes [4].

55 During avian embryonic development, the comprehensive whole mount in situ
56 hybridization expression analysis of 111 mature miRNA sequences in chicken embryos
57 revealed that miRNAs showed a variety of patterns in the early stages of development [5].
58 Tissue specific-expressed miRNAs were also found to regulate lipid metabolism and cell
59 proliferation at later stages in chicken embryonic livers [6]. Some miRNAs were extracted
60 and detected in albumen and yolk from chicken unembryonated eggs. This suggested that
61 miRNA transport from laying hens into albumen or yolk would be efficient to facilitate
62 normal embryonic development by continually supplying miRNAs to growing embryos
63 during nutrient uptake [7]. Nutrient absorption and reassembly in YSM has been confirmed
64 [2, 8]. However, the miRNA expression patterns of YSM and the crucial linkages between
65 embryos and yolk remain unclear during development.

66 The TGFβ signaling pathway is substantial in development [9]. The TGFβ family is
67 involved in paracrine signaling and can be found in different tissue types, including brain,
68 heart, kidney, liver, and sex organs. TGFβ receptor types I and II have similar ligand-
69 binding affinities and can only be distinguished by peptide mapping. Both receptor type I
70 and II have high affinities for TGFβ1, but low affinities with TGFβ2. Overall activation of
71 the TGFβ signaling pathway is through TGF family-ligand binding followed by continuous
72 phosphorylation of the type I and then type II receptor. The Smad2/3 proteins, known as

73 signal transmitters, are phosphorylated after TGFβ receptor activation. Smad4 then joins
74 with Smad2/3 to form the transcription factor complex to enter the nucleus and regulate
75 promoter regions of target genes.

76 The relationships between SOAT1 and the TGFβ signaling pathway during lipid
77 metabolism are less discussed. Although TGFβ alters cellular cholesterol metabolism in
78 smooth muscle cells by increasing LDL receptor expression and simulating substrate
79 binding (LDL), as well as enhancing delivery of cholesterol, the SOAT1 activity is not
80 changed [10]. Similarly, TGFβ increases cholesterol efflux in macrophage-derived foam
81 cells, but the SOAT1 mRNA expression (analyzed by Northern blotting) remains
82 unchanged after TGFβ stimulation [11]. However, exogenous TGFβ1 upregulates SOAT1
83 expression and activity during transition of human monocytes into macrophages [12].
84 TGFBR1 proteins are detected from early stages in chicken embryos [13]. Although the
85 Smad3 transcription factor binding region in the SOAT1 promoter is predicted by
86 Genomatix, the detailed mechanism of the TGFβ signaling pathway regulating SOAT1
87 needs to be clarified.

88 In this study, we demonstrated the miRNA profiling and miRNA-mRNA interaction
89 in primary EECs from YSM of Japanese quail. The aim of the current research was to
90 discover potential miRNAs involved in the TGFβ signaling pathway and modulation of

91 SOAT1 expression in EECs during embryonic development.

92

93 Material and methods

94 All animal studies were approved by the Institutional Animal Care and Use Committee
95 (IACUC) of the National Taiwan University. The IACUC Approval No: NTU107-EL-
96 00148.

97 microRNA sequencing

98 The microRNA sequencing of yolk sac membranes (YSM) during Japanese quail (*Coturnix*
99 *coturnix*) embryonic development was analyzed by PhalanxBio Inc. (Hsinchu, Taiwan).
100 For a better understanding of the overall miRNA expression profiles, samples of YSM were
101 collected at embryonic day 5 (ED5), ED10, ED15, and post-hatch day 2 (PH2); one sample
102 was used at each time point. Total RNA was sequenced by Illumina HiSeq2500; raw data
103 was compared with references to a chicken microRNA database, miRBase v21, for
104 comparison of miRNA precursors and mature miRNA sequences.

105

106 Prediction of microRNA targeting genes

107 Two software programs were applied to predict the unknown chicken miRNAs targeting
108 SOAT1 and the potential targets of selected miRNAs. We searched for miRNA candidates

109 that affect SOAT1 and the transforming growth factor-beta signaling pathway (TGFβ
110 signaling pathway) using miRDB (http://www.mirdb.org/miRDB/index.html) [14, 15] and
111 TargetScanHuman 7.2 (http://www.targetscan.org/vert_72/) [16]. We confirmed the
112 selected miRNAs with miRNA sequencing data. The sequences of selected miRNA are
113 listed as Table 1. SMAD3 (SMAD family member 3, a family of proteins similar to the
114 Drosophila gene 'mothers against decapentaplegic' (Mad) and the C. elegans gene Sma),
115 was one of the main signal transducers in the TGFβ signaling pathway for the SMADs
116 complex assembly and entrance into the nucleus. According to results of Genomatix
117 prediction, the SMAD3 transcription factor binding site was present in the SOAT1
118 promoter. Therefore, we hypothesized that the miRNAs affect both SOAT1 and factors in
119 the TGFβ signaling pathway.
120
121 Table 1. The list of selected miRNAs.

Chicken miRNA ID	**miRNA Sequences (5'→3')**	**Potential target sequences**	**Possible targets**
gga-miR-7455-3p	5'-CUUCCCUCCGU	5'-GTGTGCGCGCC	SMURF2, SOAT1

	CGGCGCGCACA C-3’	GACGGAGGGA AG-3’	
gga-miR-181a-5p	5’- AACAUUCAACG CUGUCGGUGA GU-3’	5’- ACTCACCGACA GCGTTGAATGT T-3’	TGFBR1, TGFBRAP1, STRAP, SMURF2, SOAT1
gga-miR-199-3p	5’- UACAGUAGUC UGCACAUUGG- 3’	5’- CCAATGTGCAG ACTACTGTA-3’	TAB2, TAB3, TGIF, SOAT1
gga-miR-133a-5p	5’- AGCUGGUAAA AUGGAACCAA AUC-3’	5’- GATTTGGTTCC ATTTTACCAGC T-3’	TGFBR1, SOAT1
gga-miR-429-3p	5’- UAAUACUGUC	5’- ACGGCATTACC	TGFBR1, SMURF2, TAB3, SOAT1

	UGGUAAUGCC GU-3’	AGACAGTATTA -3’	

SMURF2= SMAD specific E3 ubiquitin protein ligases 2

STRAP= serine/threonine kinase receptor associated protein

TGFBR1, TGFBR2= transforming growth factor beta receptor 1 or 2

TGFBRAP1= TRAP1, transforming growth factor beta receptor associated protein 1

TAB2, TAB3= TGF-beta activated kinase 1 (MAP3K7) binding protein 2, 3

TGIF= TGFB induced factor homeobox 1, TG-interacting factor 1

Validation of microRNA expressions in YSM tissues of Japanese quail

Total RNA of YSM tissues from four embryonic days were extracted by GENEzol™ Reagent (New Taipei City, Taiwan). The miRNAs were modified by polyadenylation at the 3’ end and then reverse transcribed into the cDNA of miRNA using the miScript PCR Starter Kit (#218193, Qiagen, Valencia, CA, USA) with an oligo dT primer (with a universal tag). The custom miScript Primer Assays (as forward primer, Table 2) were designed to identify different miRNAs and miScript Universal Primer was used as reverse primer. Real-time PCRs were analyzed by SensiFAST™ SYBR® Hi-ROX Kit (BIO-92020,

138 Bioline, London, UK). A PCR program was used as described: 15 minutes at 95°C, 40
139 cycles of 15 seconds at 94°C for denaturation, 30 seconds at 55°C for primer annealing, 30
140 seconds at 70°C for extension, and 1 minute at 70°C for final extension. All kits and primer
141 assays were purchased from commercial sources and were used according to manufacturer
142 instructions here and elsewhere in this manuscript.
143
144 Table 2. The miScript primer list.

Forward primer name	Sequences	Accession number on miRBase
gga-miR-7455-3p	CTTCCCTCCGTCGGCGCGCACAC	MIMAT0029065
gga-miR-181a-5p	AACATTCAACGCTGTCGGTGAGT	MIMAT0001168
gga-miR-181b-5p	AACATTCATTGCTGTCGGTGGG	MIMAT0001151
gga-miR-199-3p	TACAGTAGTCTGCACATTGG	MIMAT0003721
gga-miR-133a-5p	AGCTGGTAAAATGGAACCAAATC	MIMAT0026509
gga-miR-200a-3p	TAACACTGTCTGGTAACGATGT	MIMAT0001171
gga-miR-429-3p	TAATACTGTCTGGTAATGCCGT	MIMAT0003371
Internal control of	As forward primer,	18S ribosomal RNA

miRNA	CCGAGGCGCCUCGGUGGGC	gene (GenBank: KT445934.2)

*The reverse primer is obtained from miScript II RT Kit 10× miScript Universal Primer (Qiagen).

Cell culture system

Isolation of endodermal epithelial cells (EECs) and the culture system were modified from the published procedure [8]. In short, YSM tissues from day 5 embryos were treated with collagenase (collagenase type 4, 17104019, ThermoFisher, Waltham, MA, USA) to partially digest the extracellular matrix and facilitate cell isolation [17]. We collected six YSM (from six embryonic day five embryos) to isolate EECs; these were pooled as one sample for the experiment. EECs were cultured in DMEM/ F12 (pH 7.4, 12400–024, ThermoFisher) with 10% new born calf serum (16010–159, ThermoFisher) and 1% Penicillin-Streptomycin-Amphotericin B Solution (PSA, 03-033-1B, Biological Industries, Cromwell, CT, USA).

To emphasize functional effects, selected miRNAs were transient transfected into EECs after seeding for 48 hours. The culture medium was changed before transfection. The transfection complexes were prepared with 5 nM miRNA mimics or a 5 nM siRNA

161 negative control (AllStars Negative Control siRNA, 5'-UUCUCCGAACGUGUCACGU-
162 3') in DMEM/F12 using 3 μL HiPerFect® Transfection Reagent. The custom miScript
163 miRNA mimics, negative control, and HiPerFect® Transfection Reagent were purchased
164 from a commercial source (Qiagen).
165 The HEK293T cell line was used for validation of the target pairing between miRNAs and
166 target sequences by the luciferase reporter assay. The 293T cells were cultured in DMEM
167 (pH 7.4, 12800-017, ThermoFisher) with 10% fetal bovine serum (SH30071.02, GE
168 Healthcare Life Sciences, Utah, USA) and 1% PSA.
169

170 Real time PCR for measuring gene mRNA accumulations

171 The total RNA of YSM tissues or EECs was extracted using the GENEzol™ Reagent (New
172 Taipei City, Taiwan), followed by reverse transcription with a High Capacity cDNA
173 Reverse Transcription Kit (4368814, ThermoFisher). The cDNA was stored at -20°C. The
174 specific primers for quail gene expressions were designed by Primer3
175 (http://frodo.wi.mit.edu/primer3/) and listed below (Table 3). The reactions were prepared
176 using a SensiFAST™ SYBR® Hi-ROX Kit and 0.3 μM specific primers. The program used
177 was: 3 minutes at 95°C, 40 cycles of 5 seconds at 95°C and 30 seconds at 60°C for
178 annealing, with final extension for 1 minute at 60°C.

179

180 Table 3. The Real time-PCR primers

Primer	Source	Sequences
Gallus-β-actin-151 bp-1s	XM_015876619.1	TGGTGAAGCTGTAGCCTCTC
Gallus-β-actin-151 bp-1a		GTGATGGACTCTGGTGATGG
Quail-SOAT1-186bp-1s	XM_015869745.1	CATCCTTAATGACCGCCGGA
Quail-SOAT1-186bp-1a		ATCTGCACGTGACATGACCA
Quail-TGFBRAP1-156 bp-1s	XM_015849926.1	TCTGTTTCCCTACTGCAGCG
Quail-TGFBRAP1-156 bp-1a		CCAATCACGTTCTCCGACCA
Quail-TGFBR1-154 bp-1s	XM_015854836.1	GTTCAGGACCGGACTATGGC
Quail-TGFBR1-154 bp-1a		GCCCATCTGTCACACAGGTA
Quail-TGFBR2-129 bp-1s	XM_015853978.1	GAGAACATCCCTGCGTGGAA
Quail-TGFBR2-129 bp-1a		CCCAGCACTCGATAAGGGTC
Quail-STRAP-128 bp-1s	XM_015867774.1	ACCCCTTACGGCTACTTCCT
Quail-STRAP-128 bp-1a		TTCAACGTAGCACCCCAGAC
Quail-SMURF2-103 bp-1s	XM_015879567.1	ACATGTCCAACCAAGGGGC
Quail-SMURF2-103 bp-1a		TCAGGAAGTCGGAAAAAGTCC

Quail-TGFB2-146 bp-1s	XM_015857278.1	CAGTGGGAAGACCCCACATC
Quail-TGFB2-146 bp-1a		AAAGTGGACGTAGGCAGCAA
Quail-TGIF-124 bp-1s	XM_015855362.1	CCCAAAGAGTCCGTGCAGAT
Quail-TGIF-124 bp-1a		TGCAGACCTGTAGTGTGGAG

Luciferase plasmid construction and luciferase reporter assay

To verify the miRNA-mRNA pairing between miRNAs and 3'UTR of chicken transforming growth factor beta receptor 1 (TGFBR1, NM_204246.1), the synthetic WT sequences of the 3'UTR (Genomics, New Taipei City, Taiwan) were amplified and cloned into a pmirGLO Dual-Luciferase miRNA Target Expression Vector (E1330, Promega, Madison, WI, USA) at SacI and XhoI restriction sites. The primers used for amplifying the mutated sequence are listed as Table 4. The 3' UTR of TGFBR1 was predicted to contain two gga-miR-181a-5p binding sites and 1 gga-miR-429-3p binding site. Therefore, the synthetic mutants of TGFBR1 3'UTR were separately inserted into pmirGLO vectors. The pmirGLO-mutant-3'UTR plasmids, which had two 7 bp substitutions in the seeding regions of miR-181a-5p (MUs: TTGAATG→ GGTCCGT), and one 7 bp substitution in the seeding region of miR-429-3p (MU: TAATACT→ GCGCGCG) were all sequenced.

195 Table 4. Primers for synthetic 3'UTR amplification.

Primers	Sequences	Product size (bp)
SacI-synTGFBR1-3'UTR-1s-593bp	5'–TAAAGAGCTCTCCTGGATTTGCAACCAAAAA–3'	593
XhoI-chTGFBR1-3'UTR-1a	5'–GAAGCTCGAGATAGTTGCATAATTTATGTT–3'	

196

197 The 293T cells at a density of 3×10^4 cells/ well on 96-well plates were cultured in DMEM
198 medium with 10% fetal bovine serum and 1% PSA. When the cells reached 60% to 70%
199 confluence, pmirGLO-syn-3′UTR (100 ng) or pmirGLO-syn-mu-3'UTR-181a-5ps (100 ng)
200 or pmirGLO-syn-mu-3'UTR-429-3p (100 ng) were co-transfected with a negative siRNA
201 control or 5 to 15 nM gga-miR-181a-5p, gga-miR-199-3p, gga-133a-5p, or gga-miR-429-
202 3p mimics (Qiagen) using 0.65 μL of PolyJet™ (SL100688, SignaGen® Laboratories,
203 Rockville, MD, USA). The luciferase expression was measured by the Dual-Glo Luciferase
204 Assay System (Promega) after transfections for 24 hours, and was detected by SpectraMax
205 i3 and SoftMax Pro 7.0 (Molecular Devices, San Jose, CA, USA).

206

SDS-polyacrylamide gel electrophoresis and immunoblotting

EECs were transfected by GenMute™ siRNA Transfection Reagent (SL100568, SignaGen® Labroatories) after culturing for 48 hours. Total protein of EECs was extracted with 1X RIPA buffer (20–188, Merck, Darmstadt, Germany), supplemented with Halt™ Proteinase & Phosphatase Single-Use inhibitor cocktail (78442, ThermoFisher). Total proteins were collected by and centrifugation procedure (17000 g at 4℃ for 30 minutes) to remove mitochondria, cell membranes, nucleus and others. The supernate was stored in -80℃ for Western blotting following the previously described procedure (2). In brief, 15 μg protein/ per sample as determined using the Pierce™ BCA Protein Assay kit (23227, ThermoFisher) were subjected to 10% SDS-PAGE gel with 80V for 130 minutes, and the separated proteins were electrophoretically transferred to a polyvinylidene difluoride (PVDF) membranes (NEF1002001PK, PerkinElmer, Waltham, MA, USA) by 400 mA for 75 minutes. Nonspecific binding sites were blocked with 5% skim milk for 1 hour at room temperature. SOAT1 was detected with rabbit anti-mouse SOAT1 primary antibody (antibody diluted 1:300, orb100781, Biorbyt, Cambridgeshire, UK) followed by incubation with anti-rabbit IgG HRP-linked secondary antibody (1:5000, 7074S, Cell Signaling, Danvers, MA, USA). TGFBR1 was detected with rat anti-mouse TGFBR1 primary antibody (1:300, sc-101574, Santa Cruz, Dallas, Texas, USA) and followed by incubation

225 with anti-rat IgG HRP-linked secondary antibody (1:5000, bs-0293G-HRP, Bioss, Woburn,
226 MA, USA). The β-actin protein (1:1000, sc-4778, Santa Cruz) was detected as an internal
227 control. The target proteins were detected with the Clarity™ Western ECL Blotting
228 Substrate (#170-5061, Bio-Rad, Hercules, CA, USA). The sizes of proteins were estimated
229 with a PageRuler™ Prestained Protein Ladder (10-180 kDa) (26616LCS, ThermoFisher).
230 Protein quantifications were performed with Bio-Rad ChemiDoc Touch Imaging program.
231

232 Statistical analysis

233 All data were analyzed by one-way analysis of variance. The major effect between
234 treatments was determined by Dunnett's multiple comparison post-hoc test. The
235 significance level used was at $P \leq 0.05$.
236

237 Results

238 The discovery of candidate miRNAs involving in SOAT1
239 regulation during embryonic development

240 The aim was to find potential miRNAs for direct or indirect modulation of SOAT1
241 expression. The miRNA database for Japanese quail was not yet available, therefore, we
242 used the database from chickens (*Gallus gallus*). The miRNA lengths were mostly

243 concentrated at 22 bps (Fig 1A), and the clustering analysis showed (Fig 1B) that there
244 were 30 miRNAs with the most variance among the four developmental time points. To
245 clarify the regulation of SOAT1, two online searching tools, miRDB
246 (http://www.mirdb.org/miRDB/) and TargetScanHuman 7.2
247 (http://www.targetscan.org/vert_72/) were used to find potential miRNAs targeting
248 SOAT1. These predictions were further confirmed by miRNA sequencing data.

249 Seven miRNAs were selected and listed according to the scoring by miRDB (Table
250 1). The higher scores indicated the more confidence in prediction algorithm. They also
251 showed expression patterns according to miRNA sequencing (Fig 1C). Expressions of
252 miRNAs were further verified by real-time PCR on YSM samples (Fig 1D). The seven
253 miRNAs were gga-miR-7455-3p (MIMAT0029065; prediction score-94), gga-miR-181a-
254 5p (MIMAT0001168; score-88), gga-miR-181b-5p (MIMAT0001151; score-88), gga-
255 miR-199-3p (MIMAT0003721; score-81), gga-miR-133a-5p (MIMAT0026509; score-80),
256 gga-miR-200a-3p (MIMAT0001171; score-73), and gga-miR-429-3p (MIMAT0003371;
257 score-71).

258

259 Fig 1. Specific miRNA expressions during embryonic development of Japanese quail. Embryonic
260 day was as ED, and post-hatch day was as PH.

(A) Base pair length of miRNAs; the most frequent appearance of miRNAs was at 22 bp.

(B) Cluster analysis of miRNA sequencing. Clustering was performed to visualize the correlations among the replicates and varying sample conditions. A subset of microRNAs that exhibited the most variance was selected for cluster analysis. The number of microRNAs clustered was 250.

(C) The sequencing data set for gga-miR-7455-3p, gga-miR-181a-5p, gga-miR-181b-5p, gga-miR-199-3p, gga-miR-133a-5p, gga-miR-200a-3p, and gga-miR-429-3p. One sample was used at every time-point in the sequencing result.

(D) Confirmation of miRNA expressions by real-time PCR. Every point included seven to nine samples per group. Data were expressed as mean ± S.E.M. Statistical significance was determined by one-way analysis of variance. Dunnett's multiple comparison test was used to evaluate differences between means. A significant difference from ED5 samples was indicated as*P≤0.05, **P≤0.01, ***P≤0.005 or ****P≤0.001.

Because we only collected and analyzed one sample at each timepoint to sequence, the correlations between miRNA sequencing and real-time PCR were calculated. The results showed that the most similarity between the 7 miRNAs was with gga-miR-429-3p (about 83%), gga-miR-199-3p (61%), and gga-miR-181a-5p (50%) (Fig 2).

279 Fig 2. The correlations between sequencing and real-time PCR of gga-7455-3p, gga-miR-181a-5p,
280 gga-miR-181b-5p, gga-miR-199-3p, gga-miR-133a-5p, gga-miR-200a-3p, gga-miR-429-3p. The
281 blue lines indicated the miRNA sequencing patterns, the blue dotted lines indicated the regression
282 lines of the sequencing data, the orange lines indicated real-time PCR results and the orange dotted
283 lines indicated regression lines of the real-time PCR data.
284

285 The potential functions of selected miRNAs on regulations of
286 SOAT1 and TGFβ signaling pathway

287 We used the *ex vivo* culture system with EECs from Japanese quail YSMs, to study
288 the effects of selected miRNAs. Total RNA was extracted and analyzed after transient
289 transfection for 48 or 72 hours. The results at 48 hours showed that SOAT1 expressions
290 were decreased by gga-miR-133a-5p and by gga-miR-429-3p; furthermore, TGFBR1
291 expressions were inhibited by gga-miR-133a-5p and gga-miR-429-3p. TGFBRAP1
292 (transforming growth factor-beta receptor associated protein 1) is a specific chaperone for
293 Smad4 to bring Smad4 to phosphorylated Smad2/3 and to facilitate formation of the SMAD
294 complex [18]. STRAP (serine/threonine kinase receptor associated protein) is present in a
295 complex with Smad7 and activated TGFBR1 to stabilize the complex, and further inhibit
296 the TGFβ signaling by preventing Smad2/Smad3 access to the receptor [19]. SMURF2

297 (SMAD specific E3 ubiquitin protein ligases 2) is an E3 ubiquitin ligase and can be
298 recruited by Smad7 to form a complex to degrade TGFBR1 [20, 21].
299 Although the miRNAs were predicted to target genes mentioned above, expressions of
300 TGFBRAP1, STRAP, and SMURF2 remained unchanged after transfection (Fig 3).
301 Despite the inhibition by gga-miR-133a-5p of TGFBR1, there was no effect on SOAT1
302 after 72 hours transfection (data not shown). TGFBR1 is one of the receptors for the TGFβ
303 signaling pathway. TGFBR1 is activated and phosphorylated when TGFBR2 receives
304 ligands (e.g., TGFβ1). The downstream signals in the TGFβ signaling pathway, Smad2 and
305 Smad3 are then phosphorylated by TGFBR1. The phosphorylated Smad2/3 joins with
306 Smad4 to form the Smad complex and enters the nucleus for pairing with the transcription
307 factor binding region. Furthermore, the co-repressor (e.g., TGIF) or co-activator (e.g.,
308 CBP/p300) attaches to the complex and affects the regulations of target genes.
309
310 Fig 3. Target gene expressions after transient transfection for 48 hours using selected miRNAs.
311 Potential target gene expressions of miRNAs transfection after 48 hours were analyzed by real-
312 time PCR. C = control group with no transfection; NC = negative control group, the group of
313 transfections with AllStars Negative Control siRNA. Others = groups of miRNAs transfections (5
314 nM miRNA mimics). N= seven to eight per group. Data were expressed as mean ± S.E.M. Control

315 value was set as 1. All groups were compared with NC groups. Statistical significance was
316 determined by one-way ANOVA. Dunnett's multiple comparisons test was used to evaluate
317 differences between means (*P ≤ 0.05).
318

319 The validations of selected miRNAs pairing ability to the
320 chicken TGFBR1 3'UTR

321 To confirm the newly-found miRNA pairing abilities to 3'UTR of the target gene,
322 chicken TGFBR1, we constructed wild-type 3'UTR sequences of chicken TGFBR1 linked
323 to the luciferase expression vector (Fig 4A). After co-transfection of miRNA mimics and
324 WT-3'UTR pmirGLO plasmids into the 293T cells, the relative luciferase expressions were
325 decreased by both gga-miR-181a-5p and gga-miR-429-3p. There was no decrease by
326 gga-miR-133a-5p or gga-miR-199-3p (Fig 4B). The results suggested that gga-miR-181a-
327 5p and gga-miR-429-3p target and pair with the TGFBR1 3'UTR to inhibit TGFBR1
328 mRNA accumulation in cells. The data also suggested that gga-miR-133a-5p may not pair
329 with TGFBR1 3'UTR or pair outside the seed region or through other target genes to
330 repress TGFBR1 expression in cells.
331

332 Fig 4. The validations of selected miRNAs to chicken TGFBR1 3'UTR.

(A) The scheme of the constructed luciferase plasmid.

(B) The relative luciferase expressions after miRNA mimic transfection. Transient transfection was conducted on 293T cells ($3*10^4$ cells/ well). The pmirGLO-WT-3'UTR plasmid (100 ng) was used, and co-treated with 5 nM miRNA mimics or siRNA (negative control, NC). Firefly and Renilla luminescence were detected after transfection for 24 hours. N= nine per group. Data were expressed as mean ± S.E.M. Transfection with pmirGLO-WT-3'UTR only was set as 1. All groups were compared with NC groups. Statistical significance was determined by one-way ANOVA. Dunnett's multiple comparisons test was used to evaluate differences between means ($*P \leq 0.05$).

(C) The sequence alignment of gga-miR-181a-5p and gga-miR-429-3p with the binding sites of the chicken TGFBR1 3'UTR.

In order to clarify the conflict between gga-miR-181a-5p transfection on gene expressions and pairing ability validation, EECs were then further transfected with different miRNA concentrations. The result showed that both SOAT1 and TGFBR1 were inhibited by 15 nM miRNA (Fig 5). Therefore, TGFBR1 expression was also regulated by gga-miR-181a-5p and gga-miR-429-3p to affect SOAT1 mRNA expression in EECs.

Fig 5. Target gene expressions after transient transfection for 48 hours using gga-miR-181a-5p or gga-miR-429-3p. The expressions of SOAT1 and TGFBR1 were analyzed by real-time PCR after 48 hours of miRNAs transfection. Data were expressed as mean ± S.E.M. N= nine per group. Control group was set as 1. All groups were compared with NC groups. Statistical significance was determined by one-way ANOVA. Dunnett's multiple comparisons test was used to evaluate differences between means (*P≤0.05).

Verification of interactions between selected miRNAs and the 3'UTR of TGFBR1

The miRNA pairing activities were then further compared between the WT and the mutated 3'UTR sequences of chicken TGFBR1 (Fig 6A). To determine whether the predicted seed region of gga-miR-181a-5p and gga-miR-429-3p were true binding sites, the mutated- and WT 3'UTR of TGFBR1 were separately constructed into luciferase vectors. After transfection for 48 hours, there was no difference between WT and the seeding region mutation groups with co-transfected miRNA mimics (both gga-miR-181a-5p and gga-miR-429-3p) (Fig 6B). The data revealed that gga-miR-181a-5p and gga-miR-429-3p inhibited TGFBR1 and SOAT1 mRNA expressions by directly targeting TGFBR1 3'UTR.

Fig 6. TGFBR1 is one of the direct target gene of gga-miR-181a-5p and gga-miR-429-3p. The relative luciferase expressions after miRNA mimics transfection.

(A) Scheme of potential binding sites of gga-miR-181a-5p and gga-miR-429-3p on the wild- or mutated-type of chicken TGFBR1 3'UTR.

(B) The transient transfection was conducted on 293T cells ($3*10^4$ cells/ well). The pmirGLO-WT-3'UTR plasmid and pmirGLO-MU-3'UTR plasmid (100 ng/ well) were used and co-treated with 5 nM miRNA mimics. siRNA served as the negative control (NC). Firefly and Renilla luminescence were detected after transfection for 24 hours. N=10 to 14 per group. Data were expressed as mean ± S.E.M. All groups were compared with the NC group. Statistical significance was determined by one-way ANOVA. Dunnett's multiple comparison test was used to evaluate differences between means. A significant difference (*P≤0.05 or **P≤0.01) was indicated.

SOAT1 was regulated by gga-miR-181a-5p and gga-miR-429-3p by modulating TGFBR1 in the TGFβ signaling pathway

Protein concentrations of SOAT1 and TGFBR1 were examined after confirmation of two miRNAs pairing activity. Not only the mRNA accumulations were inhibited, but also

387 both protein expression levels were found decreased after miRNAs mimic transfection for
388 48 hours (Fig 7), suggesting that the inhibitory effects of miRNAs were effective and
389 consistent in EECs.

390

391 Fig 7. The SOAT1 and TGFBR1 protein levels after transfections with gga-miR-181a-5p or gga-
392 miR-429-3p. EECs were transfected by miRNAs mimic for 48 hours and extracted for western
393 blotting analysis. Total density of SOAT1 or TGFBR1 were normalized by total density of β-actin.
394 Data were expressed as mean ± S.E.M. N = five to nine per group. C = group of no transfection in
395 EECs, Mock = group of transfections with reagent only, NC = negative control group, the group of
396 transfections with AllStars Negative Control siRNA. Others = groups of miRNAs transfections (5
397 nM or 30 nM miRNA mimics). Control group was set as 1. All groups were compared with NC
398 groups. Statistical significance was determined by one-way ANOVA. Dunnett's multiple
399 comparison test was used to evaluate differences between means. A significant difference (*$P \leq 0.05$
400 or **$P \leq 0.01$) was indicated.

401

402 Taken together, the direct pairing ability of gga-miR-181a-5p and gga-miR-429-3p on
403 TGFBR1 3'UTR were verified by dual-luciferase assay. The expression of TGFBR1 was
404 directly targeted and attenuated by gga-miR-181a-5p and gga-miR-429-3p; therefore, the

405 TGFβ pathway was affected by miRNAs, and SOAT1 mRNA and protein levels or activity
406 was decreased. The process of cholesterol esterification was altered by miRNAs. Hence,
407 for improving avian yolk lipid regulation to enhance hatchability during embryogenesis, it
408 is very important to understand the involvement of miRNAs and miRNA expressions
409 profiles in embryonic development.
410

411 # Discussions

412 The major findings of this study are that gga-miR-181a-5p and gga-miR-429-3p both
413 had miRNA-mRNA interactions with TGFBR1 to produce inhibitory effects on TGFBR1
414 expression and regulate the TGFβ signaling pathway. In addition, the miRNAs inhibit
415 downstream target gene expression, such as SOAT1 in EECs of Japanese quail. The pairing
416 ability of two miRNAs to the complementary 3'UTR of chicken TGFBR1 was validated
417 and confirmed by the dual-luciferase reporter assay. The EECs are responsible for dynamic
418 absorption of lipids from yolk during avian embryonic development. The miRNA
419 sequencing of YSMs revealed the miRNAs involvement during avian development. We
420 demonstrated that SOAT1 is not only activated by a cAMP-dependent pathway [2], but
421 also was modulated by the TGFβ signaling pathway. The current study was the first to
422 provide direct evidence to demonstrate miRNA expression profiling in the developing

YSM of avian species.

The miRNAs are highly conserved among species. Gga-miR-181a-5p shares homology with human, mouse and zebrafish, and gga-miR-429-3p is homologous with the mouse. The very first revelation of miRNA expression patterns in avian species is by whole mount in situ hybridization from the early stages, such as ED0.5 to ED5 of chicken embryogenesis [5]. This information is further expanded by miRNA sequencing for the middle stages (ED5 to ED9, and ED11) of chicken embryogenesis [22, 23]. The miRNA patterns of chicken embryonic liver or muscle of middle and later stages are also profiled and predicted to be involved in hepatocyte proliferation/lipid metabolic pathways and to regulate muscle development [6, 24]. Nonetheless, the miRNA profiling in the extraembryonic tissues such as yolk sac membranes, are less discussed during embryogenesis in avian species.

The family of miR-181a contains four members (miR-181a/b/c/d) [25]. MiR-181a-5p has been proved to have multiple functions. In dendritic cells, miR-181a-5p reduces the immunoinflammatory response from oxidized LDL in atherosclerosis by targeting the pro-inflammatory transcription factor, c-Fos [26]. In preadipocytes, miR-181a-5p induces adipogenesis by decreasing endogenous TNFα [27], or further reduces cell proliferation through the TGFβ and the Wnt signaling pathway by directly targeting Smad7 and Tcf7l2

441 [28]. The latest results from porcine adipose tissues indicate that miR-181a-5p directly
442 targets TGFBR1 and enhances preadipocyte differentiation via PPARγ activation [29]. In
443 avian species, gga-miR-181a-5p inhibits proliferation of Marek's disease lymphoma cells
444 by targeting MYBL1 protein [30]. High concentrations of gga-miR-181a-5p are present in
445 the young chicken preadipocytes [31]. The circulating miR-181a-5p concentration is found
446 low and with negative correlations in plasma triglyceride and cholesterol in
447 hypertriglyceridemia patients. Therefore, miR-181a-5p is identified as one of the potential
448 downregulated indicators for hypertriglyceridemia [32]. According to our results and those
449 of prior studies, data strongly supports the involvement of gga-miR-181a-5p and the
450 regulation of TGFBR1.

451 MiR-429s belong to the miR-200 family of microRNAs. MiR-429-3p has the potential
452 to inhibit the Wnt signaling pathway and regulates adipogenesis though FABP4 activation
453 [33]. Hsa-miR-429 inhibits epithelial–mesenchymal transition by targeting Onecut2 in
454 colorectal carcinoma [34] and suppresses migration and invasion of a breast cancer cell
455 line [35]. In the neurodegenerative disease aspects, levels of mmu-miR-429-3p in forebrain
456 regions decrease in abundance at the clinical endpoint of prion disease [36]. The massive
457 accumulation of cholesteryl ester is observed in forebrain regions from mouse models or
458 in patients with Alzheimer's disease (AD) [37, 38], implying that SOAT1 is actively

459 involved in amyloid-β synthesis and AD formation. SOAT1 is one of the targets that may
460 have beneficial effects on AD when blocked [39], and we speculate miR-429-3p may have
461 potential relationships associated with AD.

462 In addition to the SOAT1 involvement in avian embryogenesis, one of the common
463 diseases that SOAT1 may contribute to is atherosclerosis. For many years,
464 atherosclerosis has been attributed to abnormalities in cellular cholesterol homeostasis,
465 especially in the formation of macrophage-derived foam cells [40]. One of the cytokines
466 known to participate in monocyte-macrophage differentiation, TGFβ1 increases SOAT1
467 mRNA levels in human macrophages [12]. In macrophage-derived foam cells, miR-9-5p
468 is found to target human SOAT1 mRNA 3'UTR and to reduce SOAT1 protein levels, but
469 not SOAT1 mRNA levels [41]. Another study shows that miR-467b directly targets mouse
470 SOAT1 3'UTR to regulate SOAT1 and cholesteryl ester formation [42]. However, the
471 sequences of SOAT1 3'UTR from chicken or quail are not decoded, therefore, we explored
472 the potential upstream pathway to affect SOAT1.

473 According to the real-time PCR results for two different miRNAs, gga-miR-181a-5p
474 and gga-miR-429-3p, we demonstrated that an increase in gga-miR-181a-5p levels during
475 development of Japanese quail. In contrary to gga-miR-181a-5p levels, gga-miR-429-3p
476 were shown decrease during the developmental process. However, we confirmed the

477 SOAT1 and TGFBR1 inhibitions from two miRNA by EECs primary culture system.
478 Therefore, the exact participation of gga-miR-181a-5p and gga-miR-429-3p in
479 embryogenesis requires further examination.

480 The overall scheme of predicted regulation of miRNAs and the TGFβ signaling
481 pathway with SOAT1 is illustrated in Fig 8. Taken together, embryonic SOAT1 expression
482 in YSM was regulated by gga-miR-181a-5p and gga-miR-429-3p via the TGFβ signaling
483 pathway, and TGFBR1 was the direct object of two miRNAs in Japanese quail. The current
484 research found the first indication of possible regulation mechanism of avian yolk lipid
485 utilization and modification of hatchability through changing YSM gga-miR-181a-5p and
486 gga-miR-429-3p expressions during embryonic development.

487

488 Fig 8. The possible relationship between miRNAs, TGFβ signaling pathway and SOAT1
489 expressions. The TGFβ signaling pathway is activated when the ligand (e.g., TGFβ1) binds to
490 TGFBR2, TGFBR2 phosphorylates TGFBR1. The signal transmitter Smad2/3 is phosphorylated
491 by TGFBR1 and joins with phosphorylated Smad4 to form SMAD complex in cytoplasm. The
492 SMAD complex then enters nucleus to target to transcription factor binding site to affect SOAT1
493 gene expression. However, the gga-miR-181a-5p and gga-miR-429-3p both have the inhibitory
494 ability on TGFBR1, and then decrease the SOAT1 expression. Although the gga-miR-133a-5p is

found to attenuate SOAT1 expression, the effect is independent of the TGFβ signaling pathway.

Conclusions

The expression profiles and involvements of miRNAs in the YSM of avian species were first demonstrated by microRNA sequencing technique. We further examined the biofunctions of gga-miR-7455-3p, gga-miR-181a-5p, gga-miR-199-3p, gga-miR-133a-5p, and gga-miR-429-3p using EECs primary culture system, and revealed the SOAT1 activity was attenuated by gga-miR-181a-5p and gga-miR-429-3p through directly inhibiting TGFBR1 in the TGFβ signaling pathway. This was indicative of possible regulations of avian yolk lipid utilization and modification of hatchability by changing predicted miRNA expressions.

Acknowledgements

This work was supported by the Ministry of Science and Technology, under Grant MOST 107-2313- B-002-050-MY3 in Taiwan. We especially thank the Technology Commons, College of Life Science, National Taiwan University for technical assistance on using the SpectraMax i3x Multi-Mode Plate Reader and the ultracentrifugation. We declare that the experiments comply with the current Taiwan laws, the place in which the

513 experiments were performed. There is no conflict of interest.

514

515 References

516 1. Chang TY, Chang CC, Cheng D. Acyl-coenzyme A:cholesterol acyltransferase. Annu
517 Rev Biochem. 1997; 66:613-638. doi: 10.1146/annurev.biochem.66.1.613

518 2. Wang SH, Lin HJ, Lin YY, Chen YJ, Pan YH, Tung CT, et al. Embryonic cholesterol
519 esterification is regulated by a cyclic AMP-dependent pathway in yolk sac membrane-
520 derived endodermal epithelial cells. PLoS ONE. 2017; 12(11):e0187560. doi:
521 10.1371/journal.pone.0187560

522 3. Morceau F, Chateauvieux S, Gaigneaux A, Dicato M, Diederich M. Long and short
523 non-coding RNAs as regulators of hematopoietic differentiation. Int J Mol Sci. 2013;
524 14(7):14744-14770. doi: 10.3390/ijms140714744

525 4. Kertesz M, Iovino N, Unnerstall U, Gaul U, Segal E. The role of site accessibility in
526 microRNA target recognition. Nat Genet. 2007; 39(10):1278-1284. doi:
527 10.1038/ng2135

528 5. Darnell DK, Kaur S, Stanislaw S, Konieczka JH, Yatskievych TA, Antin PB.
529 MicroRNA expression during chick embryo development. Dev Dyn. 2006;
530 235(11):3156-3165. doi: 10.1002/dvdy.20956

6. Hicks JA, Trakooljul N, Liu HC. Discovery of chicken microRNAs associated with lipogenesis and cell proliferation. Physiol Genomics. 2010; 41(2):185-193. doi: 10.1152/physiolgenomics.00156.2009

7. Wade B, Cummins M, Keyburn A, Crowley TM. Isolation and detection of microRNA from the egg of chickens. BMC Res Notes. 2016; 9:283. doi: 10.1186/s13104-016-2084-5

8. Bauer R, Plieschnig JA, Finkes T, Riegler B, Hermann M, Schneider WJ. The developing chicken yolk sac acquires nutrient transport competence by an orchestrated differentiation process of its endodermal epithelial cells. J Biol Chem. 2013; 288(2):1088-1098. doi: 10.1074/jbc.M112.393090

9. Kitisin K, Saha T, Blake T, Golestaneh N, Deng M, Kim C, et al. Tgf-Beta signaling in development. Sci STKE. 2007; 2007(399):cm1. doi: 10.1126/stke.3992007cm1

10. Nicholson AC, Hajjar DP. Transforming growth factor-beta up-regulates low density lipoprotein receptor-mediated cholesterol metabolism in vascular smooth muscle cells. J Biol Chem. 1992; 267(36):25982-25987.

11. Panousis CG, Evans G, Zuckerman SH. TGF-beta increases cholesterol efflux and ABC-1 expression in macrophage-derived foam cells: opposing the effects of IFN-gamma. J Lipid Res. 2001; 42(5):856-863.

549 12. Hori M, Miyazaki A, Tamagawa H, Satoh M, Furukawa K, Hakamata H, et al. Up-
550 regulation of acyl-coenzyme A:cholesterol acyltransferase-1 by transforming growth
551 factor-beta1 during differentiation of human monocytes into macrophages. Biochem
552 Biophys Res Commun. 2004; 320(2):501-505. doi: 10.1016/j.bbrc.2004.05.190
553 13. Cooley JR, Yatskievych TA, Antin PB. Embryonic expression of the transforming
554 growth factor beta ligand and receptor genes in chicken. Dev Dyn. 2014; 243(3):497-
555 508. doi: 10.1002/dvdy.24085
556 14. Liu W, Wang X. Prediction of functional microRNA targets by integrative modeling
557 of microRNA binding and target expression data. Genome Biol. 2019; 20(1):18. doi:
558 10.1186/s13059-019-1629-z
559 15. Wong N, Wang X. miRDB: an online resource for microRNA target prediction and
560 functional annotations. Nucleic Acids Res. 2015; 43:D146-152. doi:
561 10.1093/nar/gku1104
562 16. Agarwal V, Bell GW, Nam JW, Bartel DP. Predicting effective microRNA target sites
563 in mammalian mRNAs. Elife. 2015; 4. doi: 10.7554/eLife.05005
564 17. Lin HJ, Wang SH, Pan YH, Ding ST. Primary endodermal epithelial cell culture from
565 the yolk sac membrane of Japanese quail embryos. J Vis Exp. 2016; (109). doi:
566 10.3791/53624

18. Wurthner JU, Frank DB, Felici A, Green HM, Cao Z, Schneider MD, et al. Transforming growth factor-beta receptor-associated protein 1 is a Smad4 chaperone. J Biol Chem. 2001; 276(22):19495-19502. doi:10.1074/jbc.M006473200

19. Datta PK, Moses HL. STRAP and Smad7 synergize in the inhibition of transforming growth factor beta signaling. Mol Cell Biol. 2000; 20(9):3157-3167.

20. Kavsak P, Rasmussen RK, Causing CG, Bonni S, Zhu H, Thomsen GH, et al. Smad7 binds to Smurf2 to form an E3 ubiquitin ligase that targets the TGF beta receptor for degradation. Mol Cell. 2000; 6(6):1365-1375.

21. Xu P, Liu J, Derynck R. Post-translational regulation of TGF-β receptor and Smad signaling. FEBS Lett. 2012; 586(14):1871-1884. doi: 10.1016/j.febslet.2012.05.010

22. Glazov EA, Cottee PA, Barris WC, Moore RJ, Dalrymple BP, Tizard ML. A microRNA catalog of the developing chicken embryo identified by a deep sequencing approach. Genome Res. 2008; 18(6):957-964. doi: 10.1101/gr.074740.107

23. Hicks JA, Tembhurne P, Liu HC. MicroRNA expression in chicken embryos. Poult Sci. 2008; 87(11):2335-2343. doi: 10.3382/ps.2008-00114

24. Li T, Wu R, Zhang Y, Zhu D. A systematic analysis of the skeletal muscle miRNA transcriptome of chicken varieties with divergent skeletal muscle growth identifies novel miRNAs and differentially expressed miRNAs. BMC Genomics. 2011; 12:186.

585 doi: 10.1186/1471-2164-12-186

586 25. Su R, Lin HS, Zhang XH, Yin XL, Ning HM, Liu B, et al. MiR-181 family: regulators
587 of myeloid differentiation and acute myeloid leukemia as well as potential therapeutic
588 targets. Oncogene. 2015; 34(25):3226-3239. doi: 10.1038/onc.2014.274

589 26. Wu C, Gong Y, Yuan J, Zhang W, Zhao G, Li H, et al. microRNA-181a represses ox-
590 LDL-stimulated inflammatory response in dendritic cell by targeting c-Fos. J Lipid Res.
591 2012; 53(11):2355-2363. doi: 10.1194/jlr.M028878

592 27. Li H, Chen X, Guan L, Qi Q, Shu G, Jiang Q, et al. MiRNA-181a regulates
593 adipogenesis by targeting tumor necrosis factor-α (TNF-α) in the porcine model. PLoS
594 ONE. 2013; 8(10):e71568. doi: 10.1371/journal.pone.0071568

595 28. Ouyang D, Xu L, Zhang L, Guo D, Tan X, Yu X, et al. MiR-181a-5p regulates 3T3-L1
596 cell adipogenesis by targeting Smad7 and Tcf7l2. Acta Biochim Biophys Sin. 2016;
597 48(11):1034-1041. doi:10.1093/abbs/gmw100

598 29. Zhang Z, Gao Y, Xu MQ, Wang CJ, Fu XH, Liu JB, et al. miR-181a regulate porcine
599 preadipocyte differentiation by targeting TGFBR1. Gene. 2019; 681:45-51. doi:
600 10.1016/j.gene.2018.09.046

601 30. Lian L, Li X, Zhao C, Han B, Qu L, Song J, et al. Chicken gga-miR-181a targets
602 MYBL1 and shows an inhibitory effect on proliferation of Marek's disease virus-

603 transformed lymphoid cell line. Poult Sci. 2015; 94(11):2616-2621. doi:
604 10.3382/ps/pev289
605 31. Yao J, Wang Y, Wang W, Wang N, Li H. Solexa sequencing analysis of chicken pre-
606 adipocyte microRNAs. Biosci Biotechnol Biochem. 2011; 75(1):54-61.
607 doi:10.1271/bbb.100530
608 32. An F, Zhan Q, Xia M, Jiang L, Lu G, Huang M, et al. From moderately severe to severe
609 hypertriglyceridemia induced acute pancreatitis: circulating miRNAs play role as
610 potential biomarkers. PLoS ONE. 2014; 9(11):e111058. doi:
611 10.1371/journal.pone.0111058
612 33. Kennell JA, Gerin I, MacDougald OA, Cadigan KM. The microRNA miR-8 is a
613 conserved negative regulator of Wnt signaling. Proc Natl Acad Sci USA. 2008;
614 105(40):15417-15422. doi: 10.1073/pnas.0807763105
615 34. Sun Y, Shen S, Liu X, Tang H, Wang Z, Yu Z, et al. MiR-429 inhibits cells growth and
616 invasion and regulates EMT-related marker genes by targeting Onecut2 in colorectal
617 carcinoma. Mol Cell Biochem. 2014; 390(1-2):19-30. doi: 10.1007/s11010-013-1950-
618 x
619 35. Ye ZB, Ma G, Zhao YH, Xiao Y, Zhan Y, Jing C, et al. miR-429 inhibits migration and
620 invasion of breast cancer cells in vitro. Int J Oncol. 2015; 46:531-538. doi:

621 10.3892/ijo.2014.2759

622 36. Boese AS, Saba R, Campbell K, Majer A, Medina S, Burton L, et al. MicroRNA
623 abundance is altered in synaptoneurosomes during prion disease. Mol Cell Neurosci.
624 2016; 71:13-24. doi: 10.1016/j.mcn.2015.12.001

625 37. Chan RB, Oliveira TG, Cortes EP, Honig LS, Duff KE, Small SA, et al. Comparative
626 lipidomic analysis of mouse and human brain with Alzheimer disease. J. Biol. Chem.
627 2012; 287(4):2678-2688. doi: 10.1074/jbc.M111.274142

628 38. Tajima Y, Ishikawa M, Maekawa K, Murayama M, Senoo Y, Nishimaki-Mogami T, et
629 al. Lipidomic analysis of brain tissues and plasma in a mouse model expressing mutated
630 human amyloid precursor protein/tau for Alzheimer's disease. Lipids Health Dis. 2013;
631 12:68. doi: 10.1186/1476-511X-12-68

632 39. Shibuya Y, Chang CC, Chang TY. ACAT1/SOAT1 as a therapeutic target for
633 Alzheimer's disease. Future Med Chem. 2015; 7(18):2451-2467. doi:
634 10.4155/fmc.15.161

635 40. Hansson GK, Robertson AK, Söderberg-Nauclér C. Inflammation and atherosclerosis.
636 Annu Rev Pathol. 2006; 1:297-329.

637 41. Xu J, Hu G, Lu M, Xiong Y, Li Q, Chang CC, et al. MiR-9 reduces human acyl-
638 coenzyme A:cholesterol acyltransferase-1 to decrease THP-1 macrophage-derived

639 foam cell formation. Acta Biochim Biophys Sin. 2013; 45(11):953-962. doi:
640 10.1093/abbs/gmt096
641 42. Wang B, He PP, Zeng GF, Zhang T, Ouyang XP. miR-467b regulates the cholesterol
642 ester formation via targeting ACAT1 gene in RAW 264.7 macrophages. Biochimie.
643 2017; 132:38-44. doi: 10.1016/j.biochi.2016.09.012

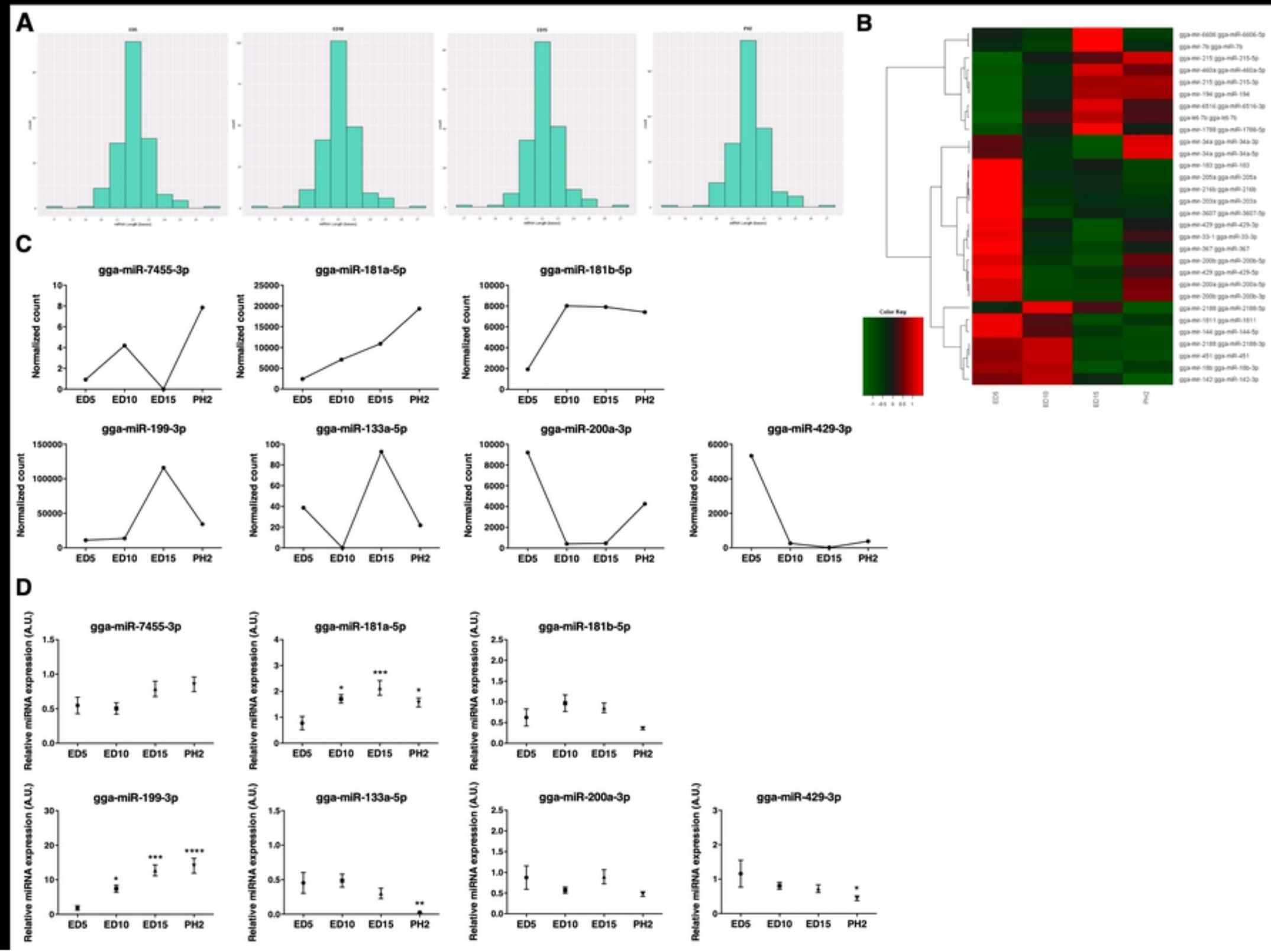
A
B
C
gga-miR-7455-3p
gga-miR-181a-5p
gga-miR-181b-5p
gga-miR-199-3p
gga-miR-133a-5p
gga-miR-200a-3p
gga-miR-429-3p
Normalized count
ED5
ED10
ED15
PH2
D
Relative miRNA expression (A.U.)

Fig 1

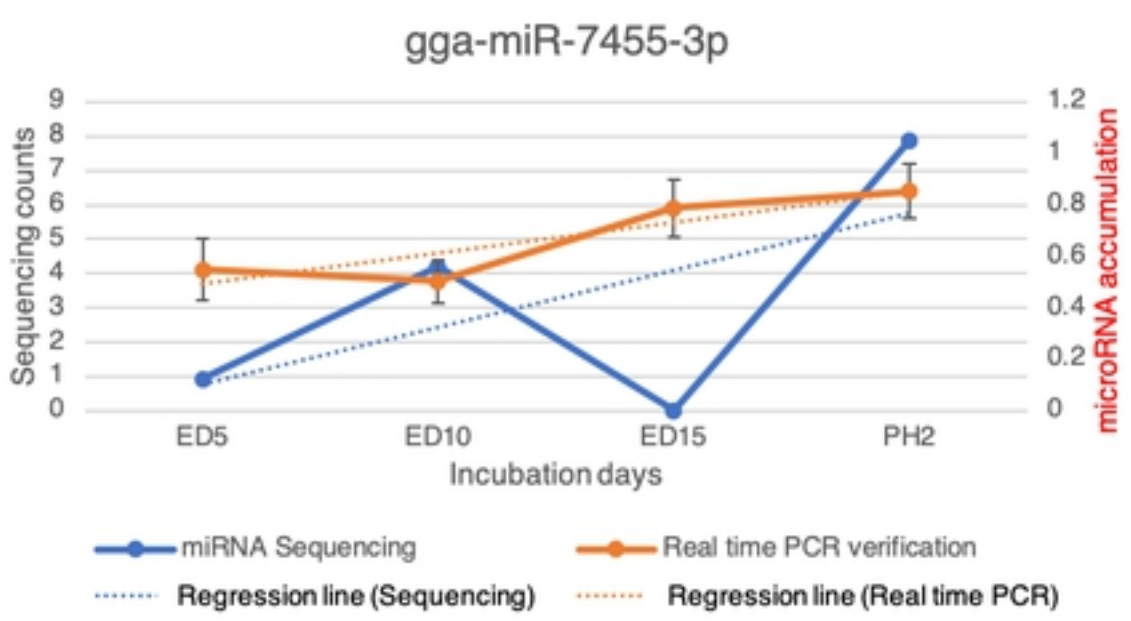

Correlation=0.31757121

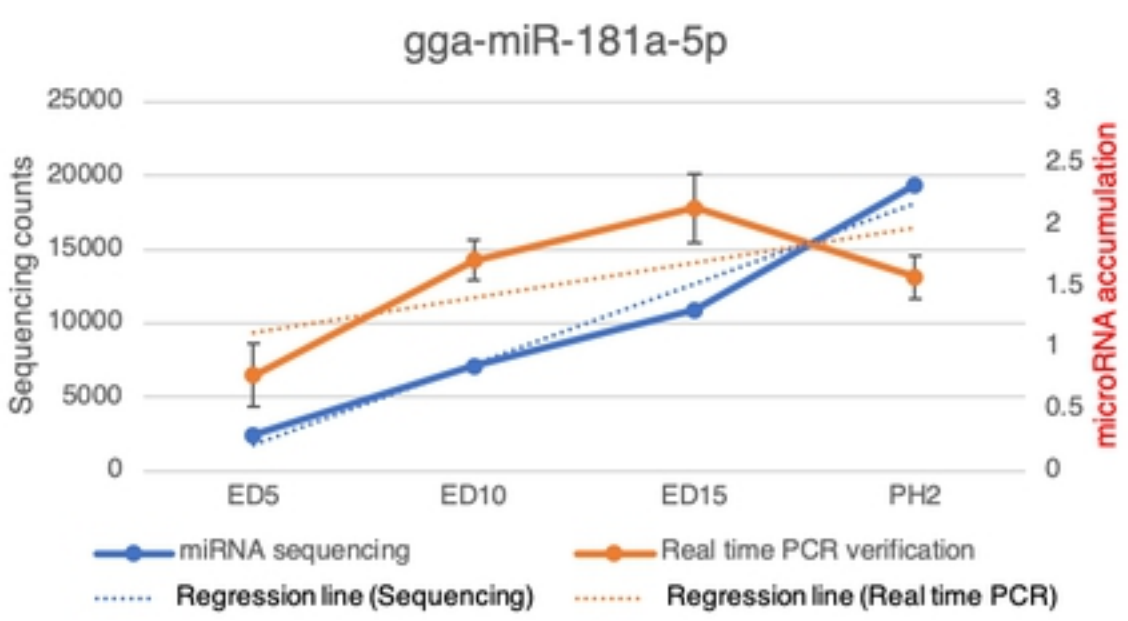

Correlation= 0.503335736

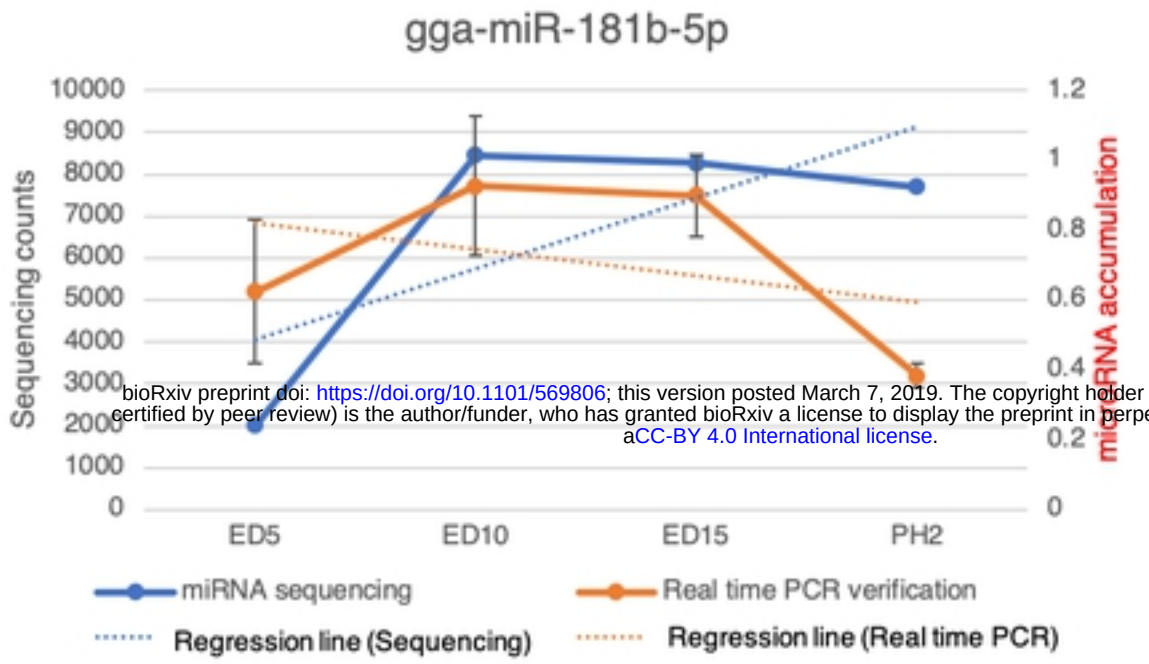

Correlation= 0.316287108

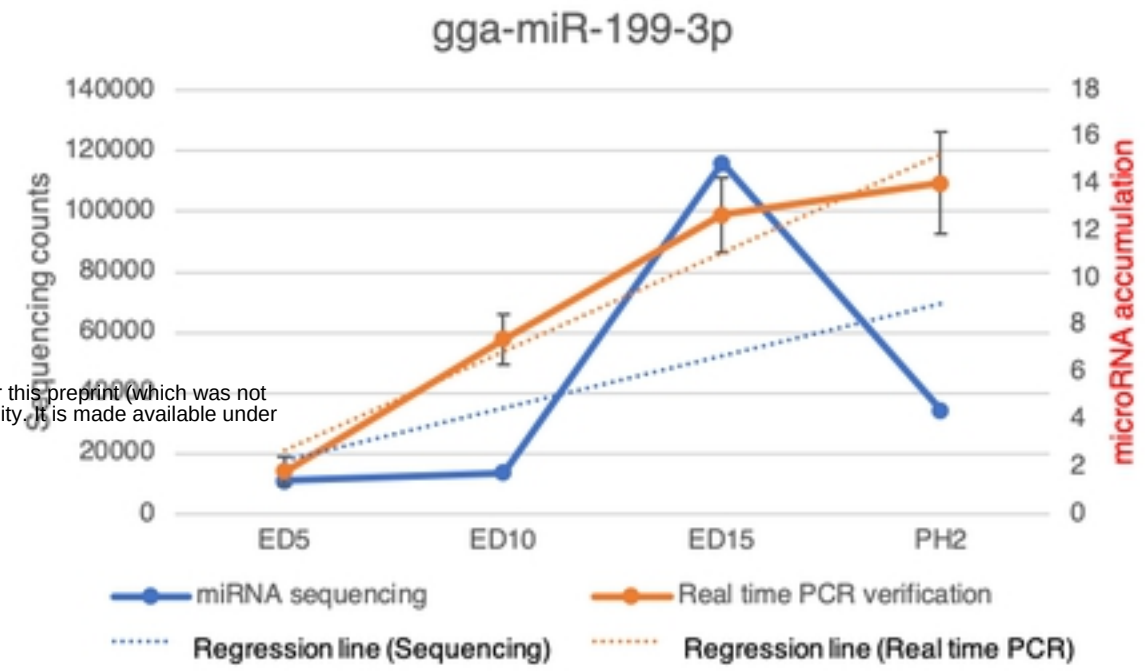

Correlation= 0.610143255

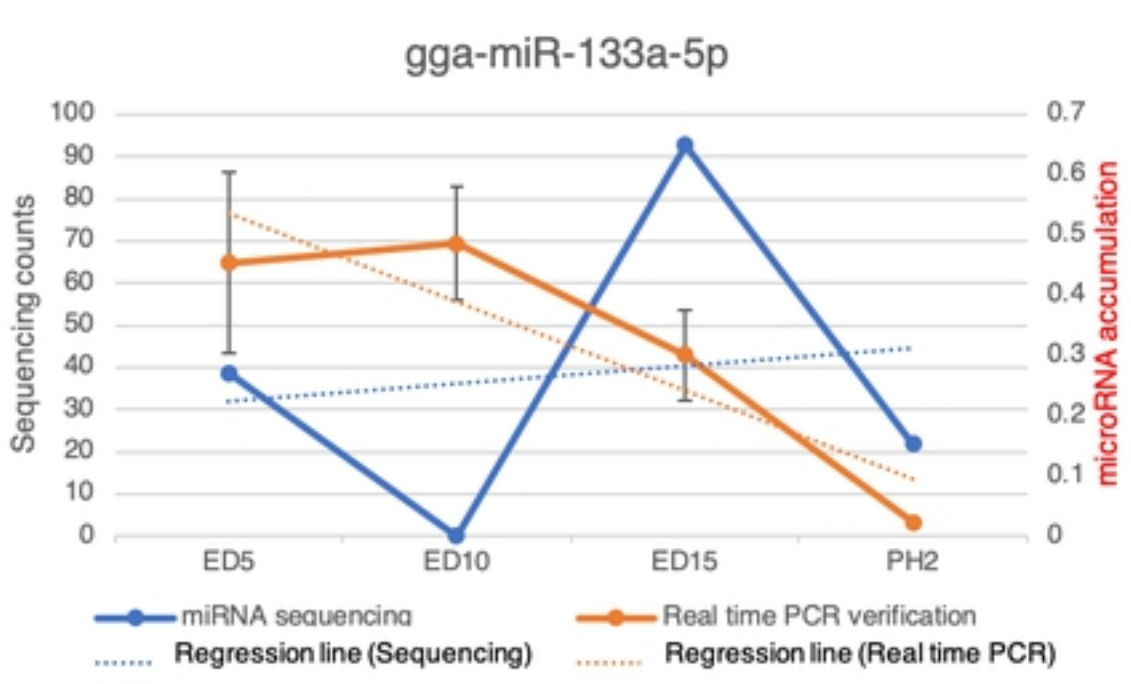

Correlation= -0.09684383

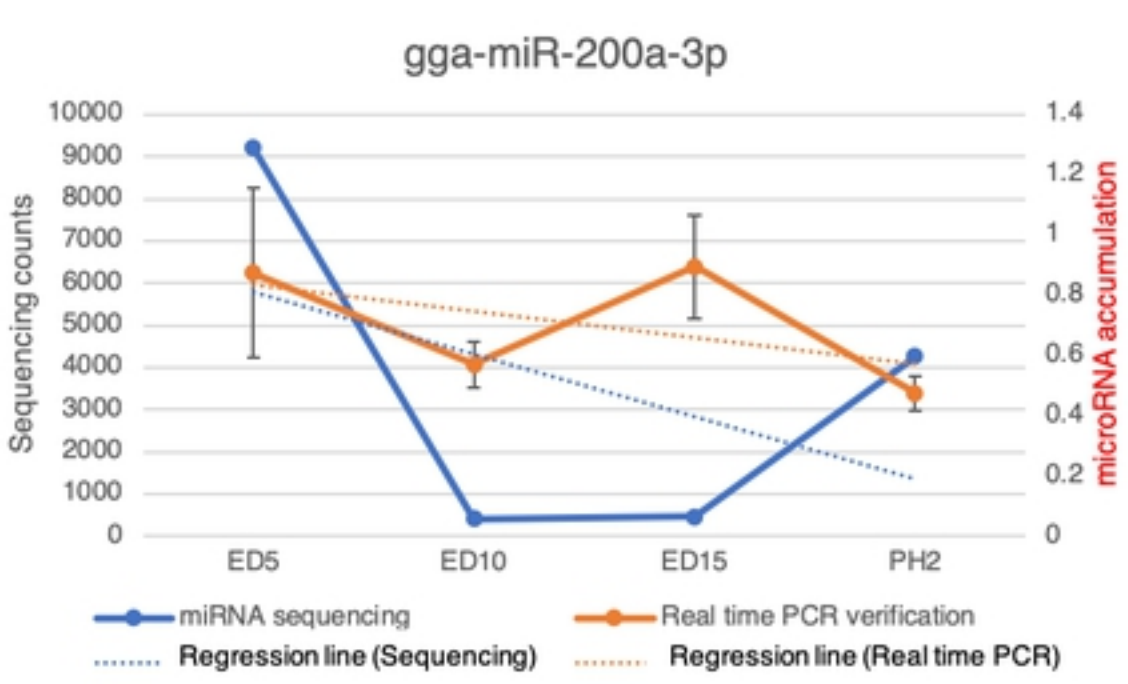

Correlation= 0.238084732

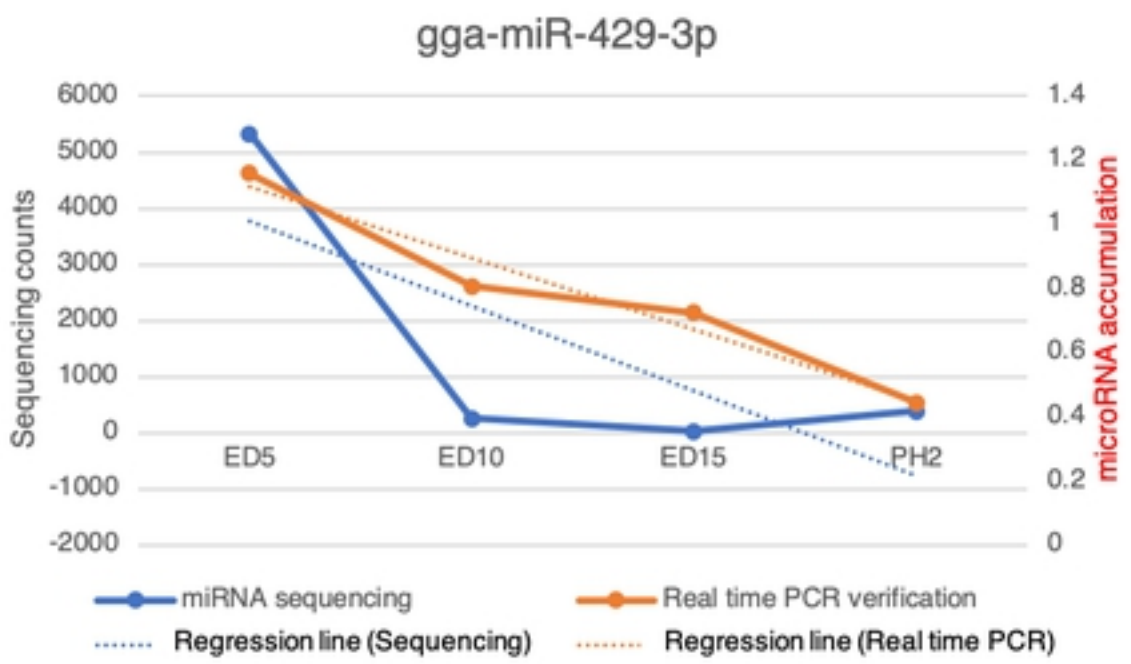

Correlation= 0.831176843

Fig 2

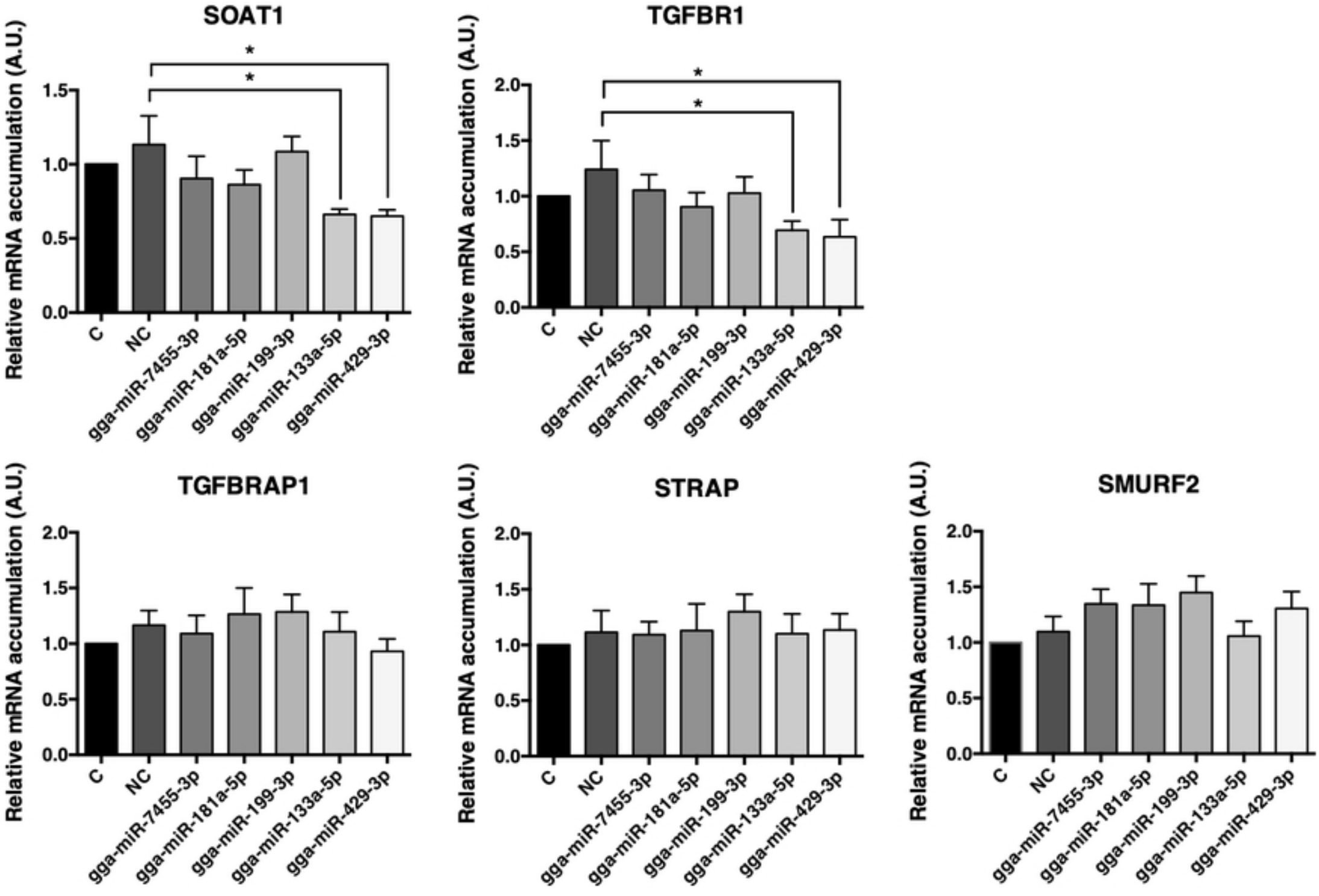
SOAT1
TGFBR1
TGFBRAP1
STRAP
SMURF2
Relative mRNA accumulation (A.U.)
0.0
0.5
1.0
1.5
2.0
*
*
C
NC
gga-miR-7455-3p
gga-miR-181a-5p
gga-miR-199-3p
gga-miR-133a-5p
gga-miR-429-3p

Fig 3

A

PGK promoter	*luc2*	3'UTR of TGFBR1 (573bp)	SV40 poly(A)	SV40 early promoter	*hRluc*-neo fusion	Synthetic poly(A)

B

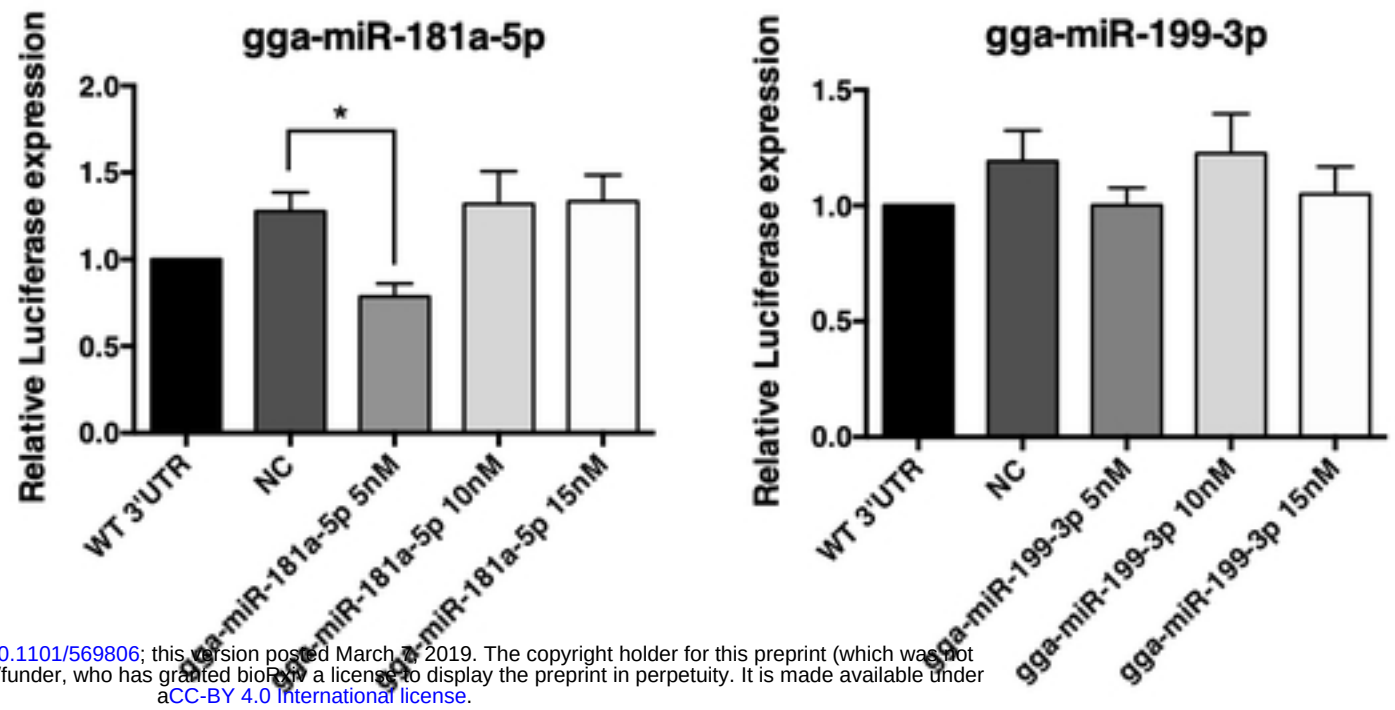

C

Mouse 5'- · · · TTGGTTCAC––T**TTGAATG**TACTGTT · · · -3'

WT 3'UTR TGFBR1

Human 5'- · · · TTGATTCAGACT**TTGAATG**TACTGTT · · · · · · CTTA**T**AA**AA**CTCTTA · · · -3'

Chicken 5'- · · · TTGATTCAGATT**TTGAATG**TACTGTT · · · · · · CTT–**TTGAATG**CTTA · · · -3'

gga-miR-181a-5p 3'-UGAGUGGCUGUCGC**AACUUAC**AA-5' 3'- · · · UCGC**AACUUAC**AA-5'

1st seed region
Position: 456 – 462 bp

2nd seed region
Position: 507 – 513 bp

WT 3'UTR TGFBR1 Chicken 5'- · · · · · ATTGCTGCCTTTT**TAATACT**TCATAGG · · · -3'

Complementary Strand 3'- · · · · TAACGACGGAAA**ATTATGA**AGTATCC · · · · -5'

gga-miR-429-3p 5'–**UAAUACU**GUCUGGUAAUGCCGU–3'

Position: 126 – 132 bp

Fig 4

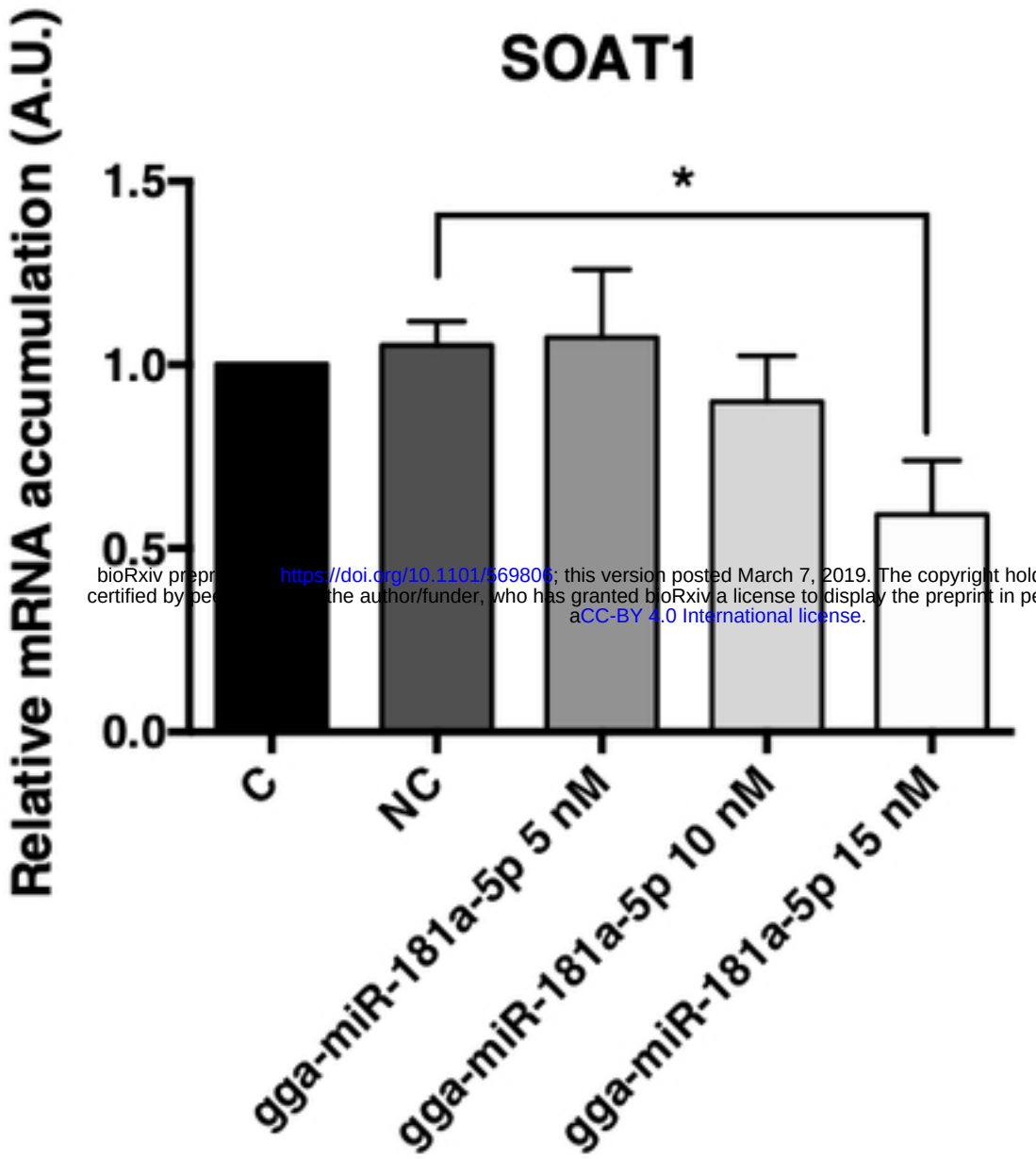

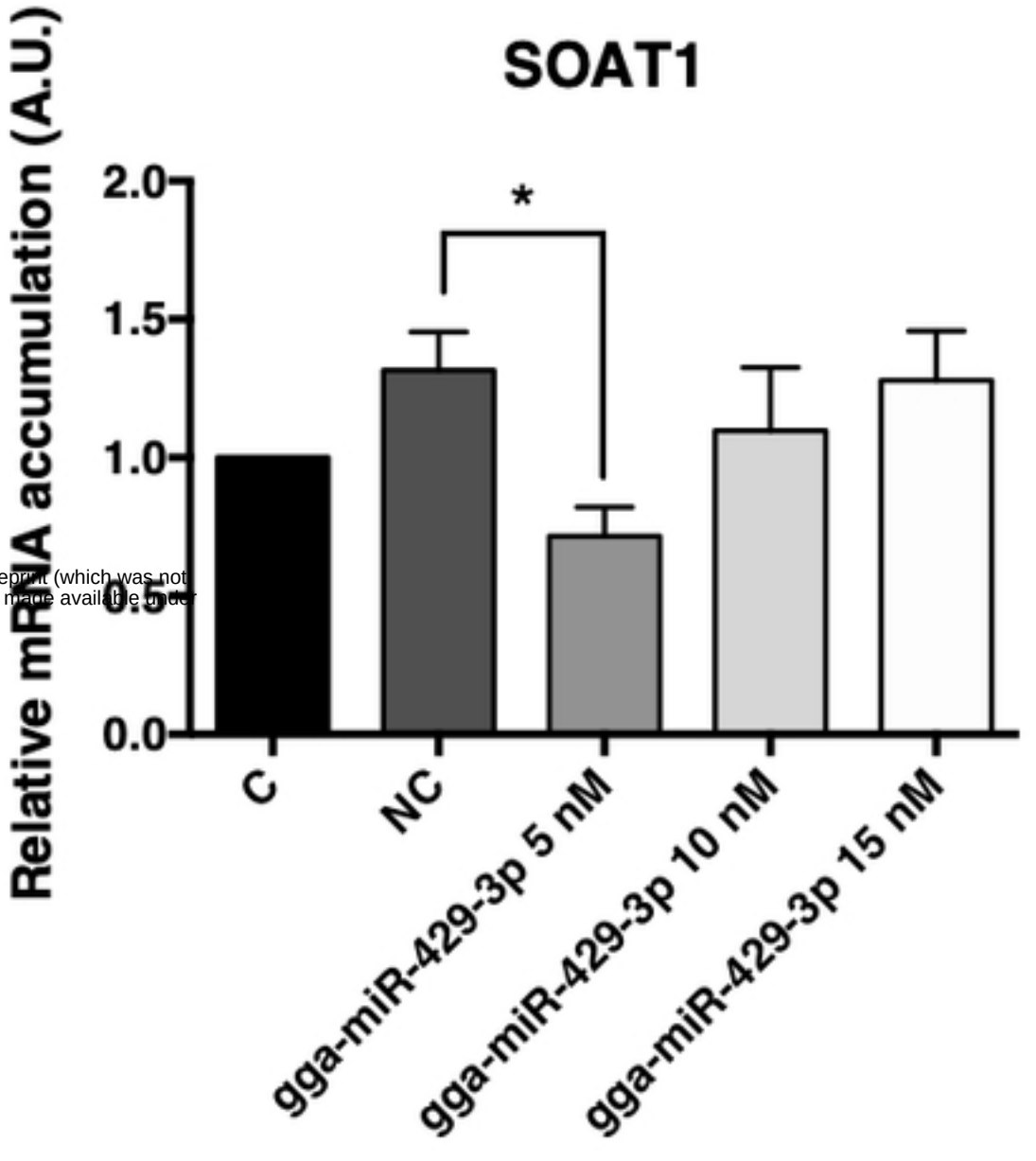

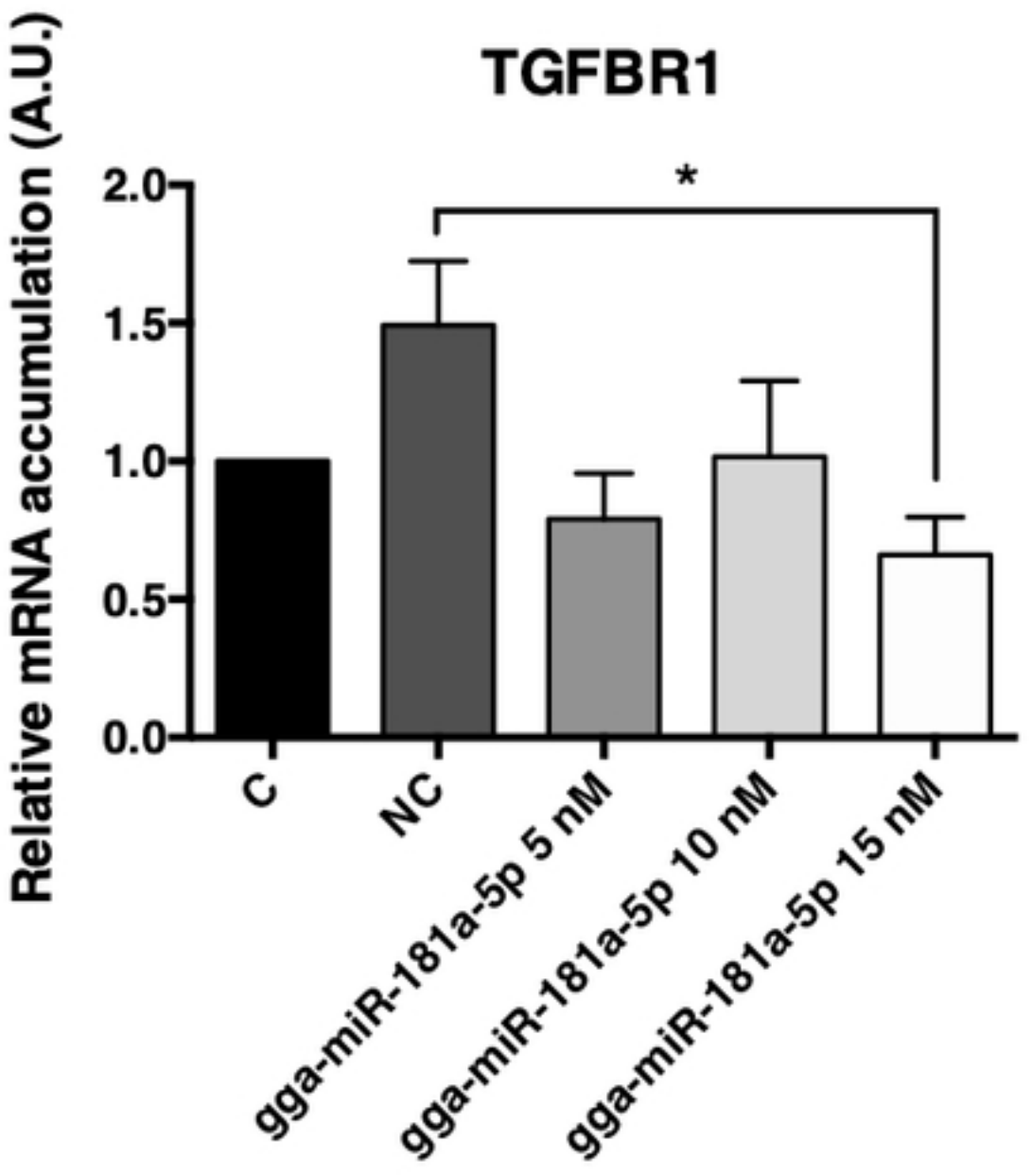

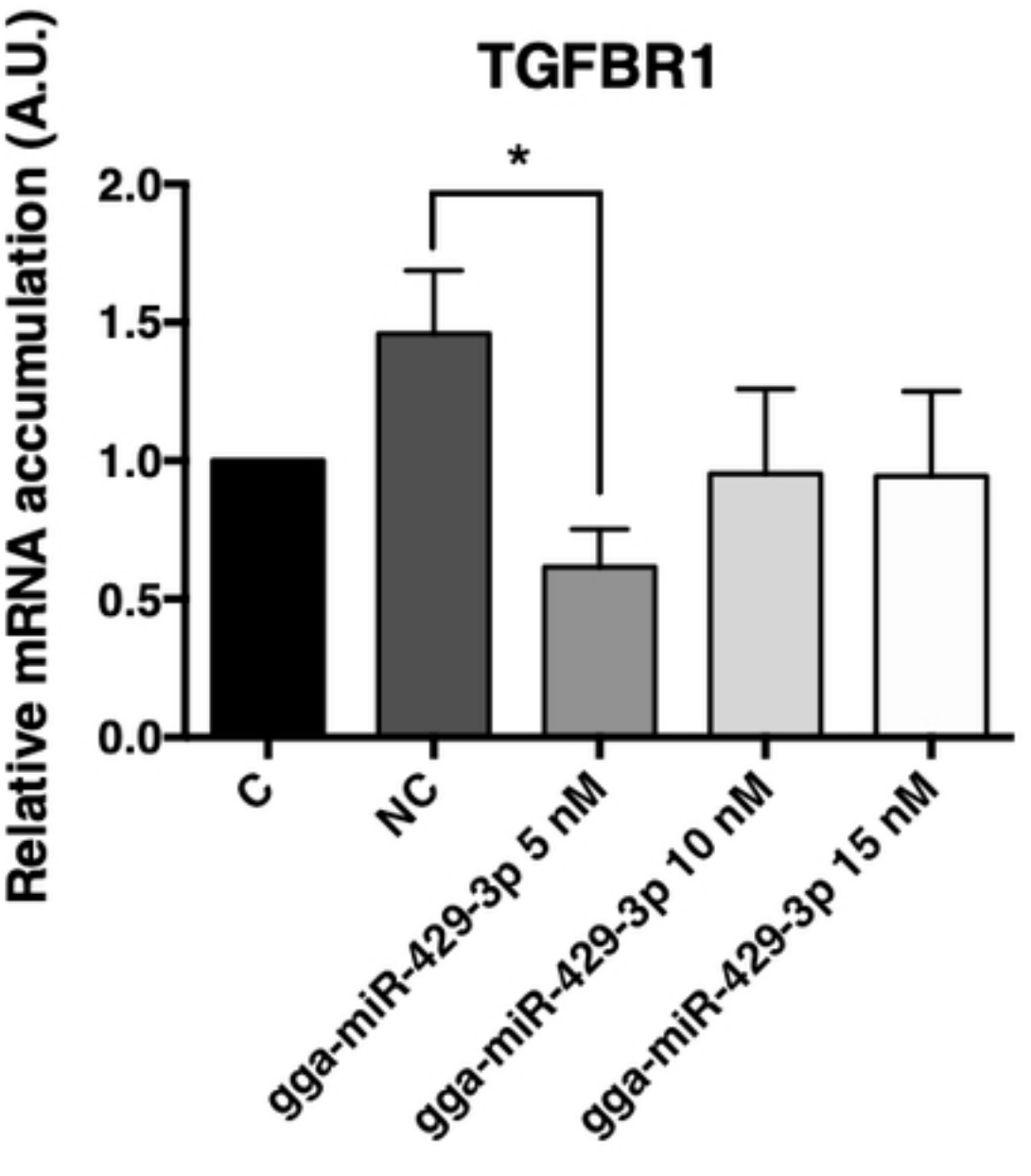

Fig 5

A

WT Chicken 3'UTR 5'- · · · · TTGATTCAGATTGGTCCGTTACTGTT · · · · · · CTT**TTGAATG**CTTA · · · -3'

Mutated 3'UTR 5'- · · · TTGATTCAGATTGGTCCGTTACTGTT · · · · · · CTTGGTCCGTCTTA · · · -3'

gga-miR-181a-5p 3'-UGAGUGGCUGUCGC**AACUUAC**AA -5' 3'- · · · UCGC**AACUUAC**AA-5'

1st seed region
Position: 456 – 462 bp

2nd seed region
Position: 507 – 513 bp

WT Chicken 3'UTR 5'- · · · · · ATTGCTGCCTTT**TAATACT**TCATAGG · · · -3'

Mutated 3'UTR 5'- · · · · · ATTGCTGCCTTTGCGCGCGTCATAGG · · · -3'

Mutated complementary strand 3'-· · · · · TAACGACGGAAACGCGCGCAGTATCC · · · -5'

gga-miR-429-3p 5'- **UAAUACU**GUCUGGUAAUGCCGU -3'

Position: 126 – 132 bp

B

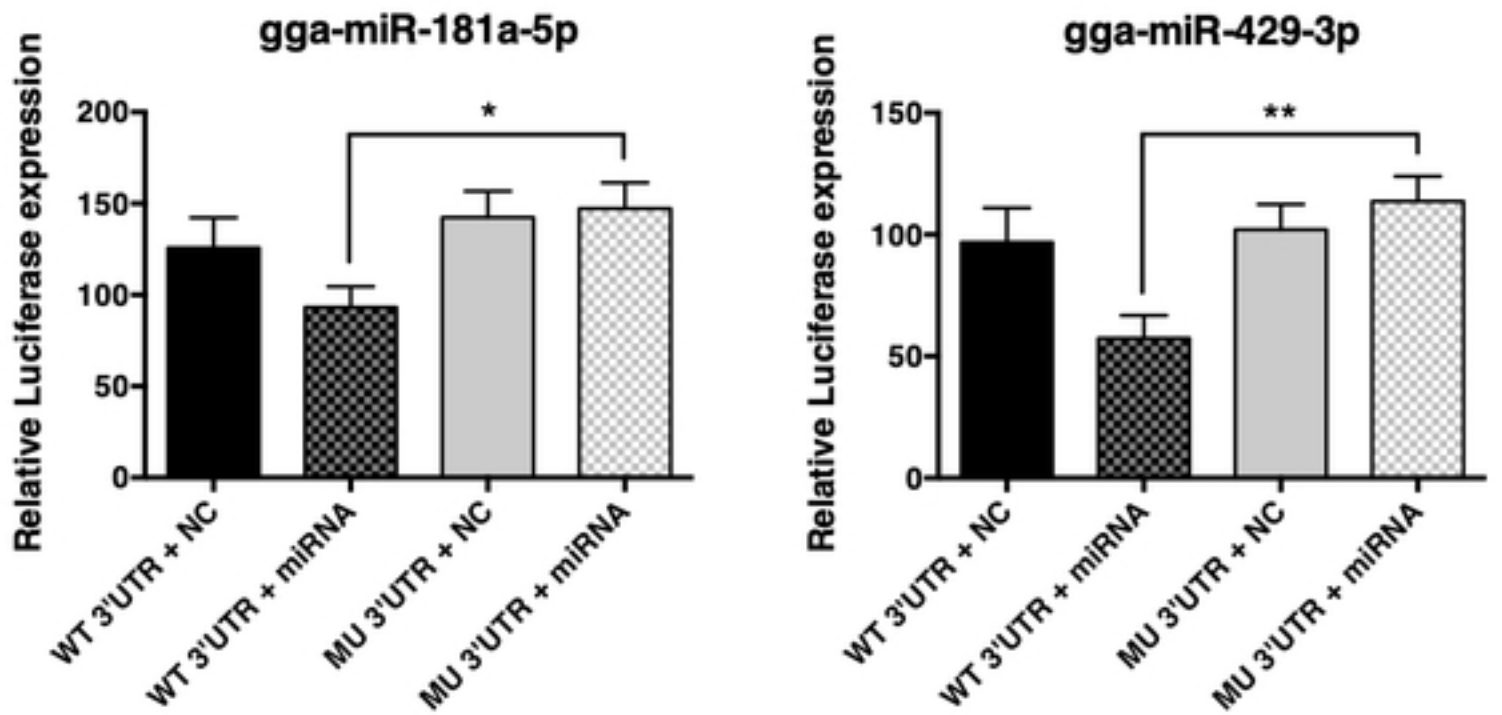

Fig 6

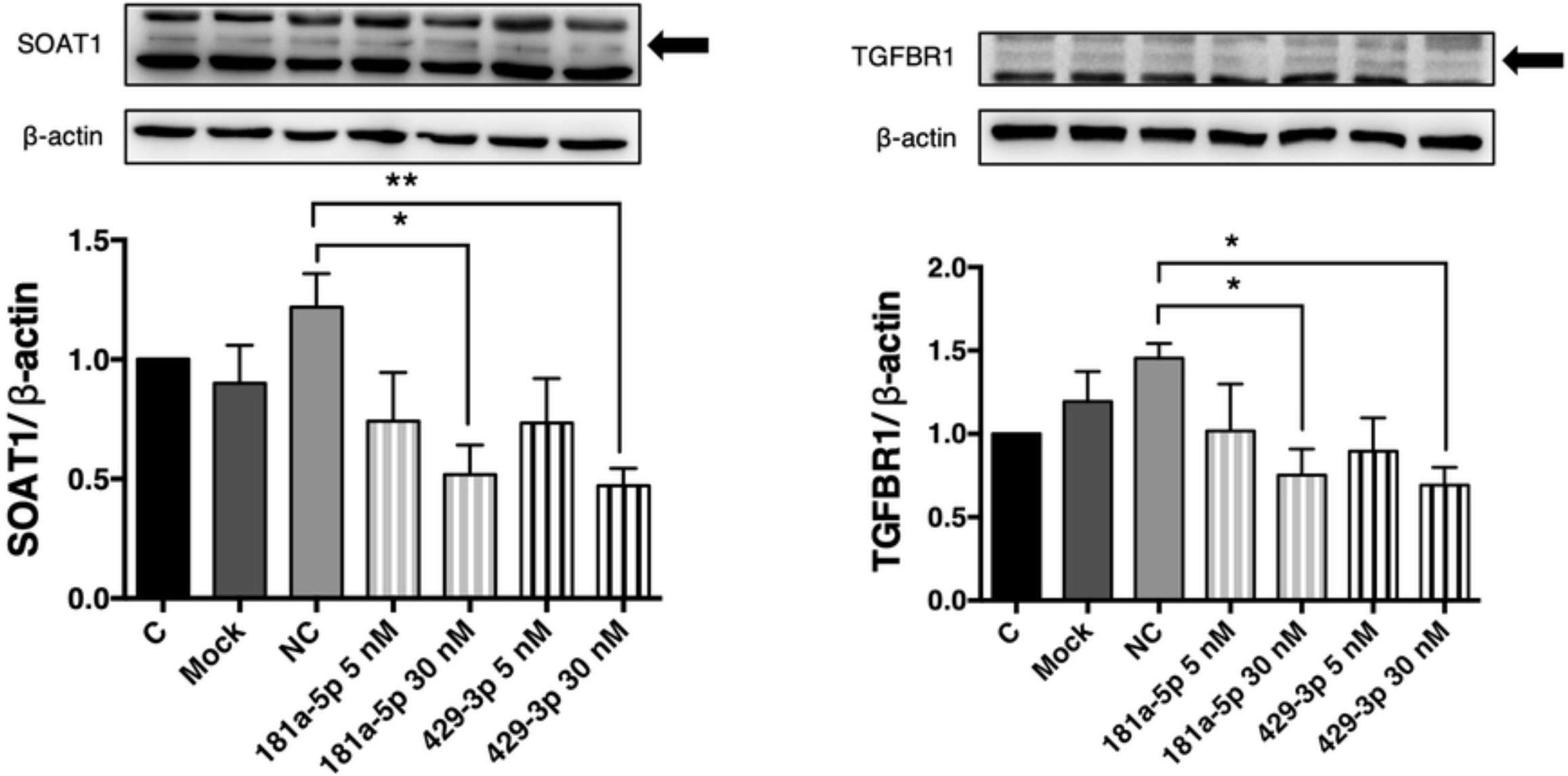
SOAT1
β-actin
**
*
SOAT1/β-actin
1.5
1.0
0.5
0.0
C
Mock
NC
181a-5p 5 nM
181a-5p 30 nM
429-3p 5 nM
429-3p 30 nM
TGFBR1
β-actin
*
*
TGFBR1/β-actin
2.0
1.5
1.0
0.5
0.0
C
Mock
NC
181a-5p 5 nM
181a-5p 30 nM
429-3p 5 nM
429-3p 30 nM

Fig 7

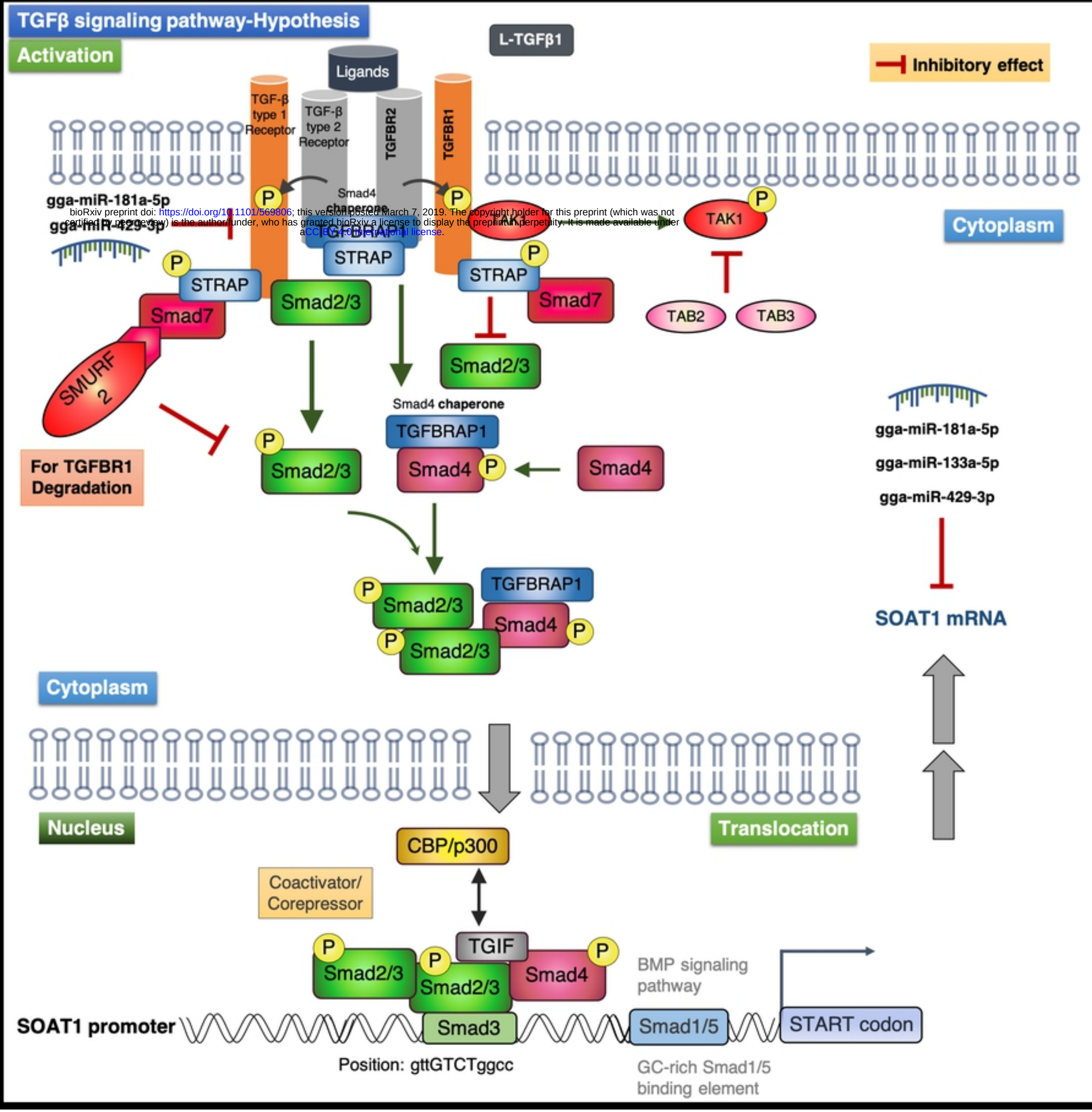

Fig 8